

Recent advances and biophysical applications of atomic force microscopy in cancer research: An overview

Bharath Sampath Kumar^{*1,†}

*1 Independent researcher, 21, B2, 27th street, Nanganallur, Chennai 61, India.

† Correspondence should be addressed to: 21,27th street, B2, Lakshmi Flats, Nanganallur, Chennai 61, India. (e-mail: bskumar80@gmail.com).

Abstract: The implementation of atomic force microscopy (AFM) in cancer detection investigations has been made possible by new developments. Living cells' physical and chemical characteristics fluctuate anytime their physiological environments are modified. Consequently, such physical and chemical traits may represent intricate biological functions happening within cells. The shape, flexibility, and adhesive characteristics of cells can alter while they are going through the tumorigenesis phase and are driven by environmental factors. In settings that are close to physiological, AFM can carry out surface mapping and ultrastructural characterization of live cells with atomic-level resolution, as well as capturing force spectroscopy data that enables the investigation of the mechanical characteristics of cells. As a result, high resolution studies concerning the structure and mechanical attributes of cancer cells may benefit from the application of AFM. The principles of operation theory, mode of operation, and technical characteristics of AFM are presented in this paper, along with its various applications and future possibilities in cancer studies.

Keywords: AFM, carcinoma, Raman spectroscopy, hybrid AFM imaging,

1. Introduction

Cancer is one of the top causes of death worldwide. When this condition manifests, cancer cells develop abnormal properties, such as the ability to continuously proliferate and generate metastases, i.e., thereby leaving localized tissue to propagate via blood vessels to various adjacent organs and invade them. When compared to the healthy cells from which they have been derived, cancer cells' chemical and physical properties are distinct since they are unrestrained and quickly reproducing cells.¹⁾ To accommodate the biological functions of tumor cells themselves, throughout growth and dissemination, the degree of adhesion among cells diminishes, and the form and stiffness of the cells themselves alter in accordance with the immediate surroundings.²⁻⁴⁾ Consequently, using physical features like stiffness, adherence, and Young's modulus, investigators can ascertain the likelihood that cells are malignant, if cancerous cells are intrusive or metastasizing, and the impact of medications on tumor cells, among other factors.⁵⁾ Nevertheless, to carry out the previously mentioned studies, it is essential to examine

and experiment with cells at a spatial resolution of a few nanometers.

There has been a significant rise in interest during the past decade in the mechanical study of biological specimens within the confines of diseases.⁶⁾ As a result, several approaches to examining tissue and cell mechanics have been refined and developed. Among these methods are optical tweezers,⁷⁾ magnetic twisting cytometry,⁸⁾ optical stretching,⁹⁾ and AFM,¹⁰⁾ although these methods are by no means the only options. AFM is a very high-resolution instrument that may be used to analyze a sample's morphology and quantitatively assess its mechanical characteristics down to the atomic level.⁶⁾ Hence, AFM can be employed in cancer studies. AFM surpasses the resolution limitations of light and electron microscopes with a vertical as well as horizontal resolution of 0.1 nm. AFM employs a miniature physical probe to gather information derived from the interaction between the probe and the specimen's surface to examine the morphology of the material under inquiry in three dimensions.⁶⁾

The key factors behind AFM's swift and broad acceptance in medical and biological research happen to be its technical benefits.¹¹⁾ First and foremost, because of AFM's extraordinarily excellent resolution, molecular- as well as atomic-scale features may be directly imaged in three dimensions.⁵⁾ Second, the sampling process for AFM is simple, there is minimal damage to the original structure, and the specimen's original appearance may be precisely and objectively assessed.⁵⁾ In third place, the ever-changing actions of molecules, organelles, and additional elements in living cells can be captured in actual time by AFM since specimens can be observed in nearly physiological conditions.¹²⁾ In the fourth position, the forces between molecules, charge, pH, and other physical and chemical characteristics of samples can all be measured using AFM.⁵⁾ The customized probe can also be utilized to pinpoint certain molecules or forces of interaction, like ligand-receptor interactions. As a result of the above-mentioned qualities, AFM has an increased likelihood of being used in clinical research, especially in the identification and management of cancer.^{13,14)} AFM can differentiate among several cancerous cell stages in addition to differentiating between normal and malignant cells depending on their distinct mechanical features.¹⁵⁾ For instance, the AFM can separate different human colon carcinoma cell lines based on rigidity characteristics that tend to be inversely correlated to neoplastic severity when combined with machine learning and visualization.¹⁶⁾ It is possible to determine the kind of programmed cell death mechanism that rodent fibrosarcoma cells undergo using nano topographical investigation and mechanical analysis by AFM.¹⁷⁾

Experiments conducted *in vitro* frequently fall short of capturing the diverse characteristics of a malignant condition and its host organ.^{17,18)} Indeed, tissues serve as more suitable research tools for a variety of mechanopathology-related problems. Cancerous tissues are frequently harder owing to elevated extracellular matrix accumulation and cross-linking, even though cancerous cells are normally more flexible compared to their healthy equivalents.^{13,17)} Indeed, enhanced rigidity of tissues has been associated with tumor growth and is a recognized cancer characteristic.¹⁹⁾ This is attributable to some extent to cells' capacities for mechanoreception and mechanotransduction, which allow them to detect and react to tangible signals in their surroundings. Mechanoresponsive pathways of communication are consequently triggered to assist in survival and growth when cancer cells are exposed to the abnormal

mechanical conditions found in the microenvironment associated with tumors.²⁰⁾ To completely comprehend how cell mechanics drive carcinogenesis, metastasis, and medication resistance, it remains crucial that these kinds of biomechanical mechanisms and relationships be maintained and investigated in situ.⁶⁾ AFM's unique capacity to obtain mechanical characteristics from biological substances and correlate them to the progression of cancer may help uncover novel options for research and application in the clinic, even though assays like immunohistochemistry and immunofluorescence are not as technically demanding.^{13,21)} Nevertheless, even though AFM based techniques are gaining popularity, little investigation has been done employing AFM-based approaches on cancer and cancer-bearing tissues.

The physical characteristics of cancer have not been thoroughly studied. AFM could potentially be utilized to explore alterations to the structure and mechanical characteristics of cancer cells and tissues because of its many distinctive benefits, which can then be employed as a foundation for clinical diagnostics.²²⁾ AFM also makes it possible to investigate the cellular and molecular pathways by which anticancer medications work, allowing for the assessment of their effectiveness and providing new opportunities for the prevention of the proliferation of tumor cells.²³⁻²⁷⁾ The principles of operation theory, mode of operation, and technical characteristics of AFM are presented in this paper, along with its various applications and future possibilities in cancer studies. Table 1 presents information about tumor type, supplementary techniques employed, contact mode, mechanics model, tip radius, spring constant and scan velocity.

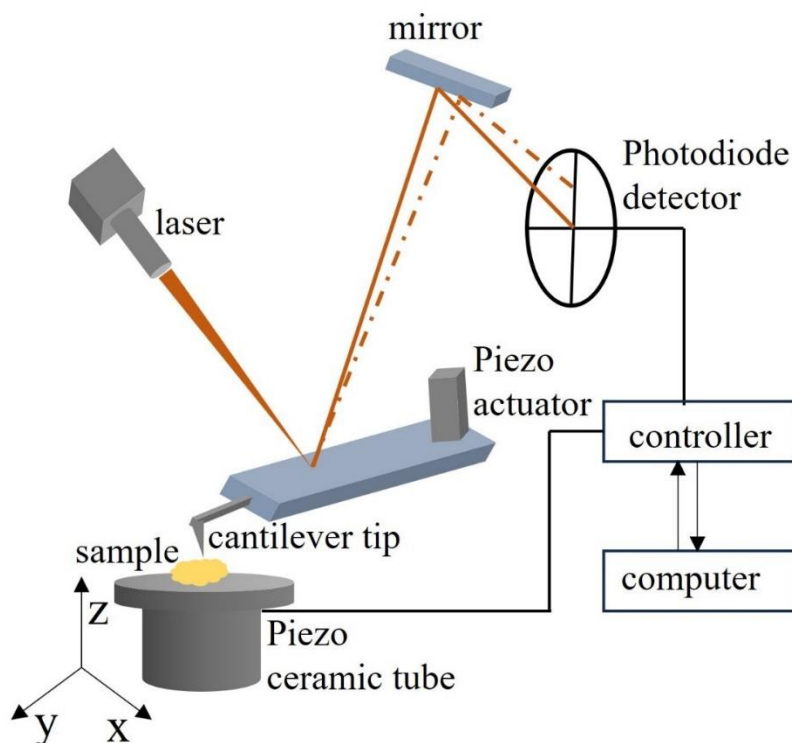


Fig. 1. AFM working principle.

Table 1. Empirical studies on AFM in cancer research

Author	Tumor type	ST	Mode	CMM	TM	SC N/m	SV
Van der Meeren et al (2020)	Apoptosis, Necroptosis, and Ferroptosis in Murine Cancer Cells	Immunofluorescence imaging	Contact	Hertz	5µm & 30nm	0.1 & 0.06	2µm/s
Silva et al (2022)	Pancreatic cancer	Two photon Fluorescence	Contact	Hertz	6nm	0.02 & 3	2µm/s
Curci et al (2022)	Inflammatory Bowel Disease	ELISA	Contact	NR	10nm	0.6-2	1Hz
Chen et al (2021)	Breast cancer	bioluminescent H&E staining	imaging & Contact	Hertz-Sneddon	25µm	0.02	5µm/s
Azzalini et al (2021)	Ovarian cancer	HE Stain	Contact	Hertz	20	3.5	NR
Deliorman et al (2022)	Prostate cancer	Immunostain	Contact	Hertz	NR	0.01-2	4
Raudenska et al (2019)	Prostate cancer	qRT-PCR	Contact	Hertz-Sneddon	NR	1	30
Alhalhooly et al (2021)	brain, breast, prostate, and pancreatic cancer	FM	Contact	Hertz	NR	0.08	3µm/s
Chen et al (2021)	Breast cancer	Confocal microscopy	Contact	Hertz	2.6µm	0.02-0.77	2µm/s
Tang et al (2022)	Prostate cancer	Confocal microscopy	Contact	Hertz	NR	0.01	2µm/s
Zbiral et al (2021)	Breast cancer	Confocal microscopy	Contact	Hertz-Sneddon	10nm	0.12	0.5-0.8Hz
Chen et al (2020)	Ovarian cancer	Confocal microscopy	Contact	Hertz	NR	0.01	5µm/s
Paul et al (2020)	Colon cancer	FT-IR, CD, RS	Tapping	Hertz	default	0.03	0.5lines/s
Zhu et al (2021)	liver and lung cancer	Cell viability assay	Contact	Hertz-Sneddon	20nm	0.07	2µm/s
Barai et al (2021)	cancer cells	NA	Contact	Hertz	10µm	0.06	5µm/s
Levillain et al (2022)	breast, kidney, and thyroid tumor	H&E Stain	Contact	Hertz-Sneddon	NR	0.01-0.03	2µm/s
Brás et al (2022)	Colorectal cancer	Immunostain	Contact	Hertz	75nm	default	2Hz
Contessoto et al (2021)	Cervical cancer	NA	Contact	Hertz	NR	0.01	3µm/s
Kim et al (2019)	murine mammary carcinoma	NA	Contact	Hertz	10µm	0.05-0.08	5µm/s
Yurtsever et al (2021)	Osteosarcoma	ELISA	Contact	Hertz-Sneddon	7.2µm	0.126	15µm/s
Deptula et al (2020)	Colon cancer	H&E Stain	Contact	Hertz	4.5µm	0.4-0.6	1Hz

NR – not reported; CMM – contact mechanics model; TM – tip measurement; SV – scan velocity; ST- supplementary techniques; SC – spring constant

2. AFM working principle

The AFM system is made up of a piezoelectric ceramic scanning [PCS] system, a micro-cantilever equipped with a probe, a movement recognition system to detect the micro-cantilever, a feedback mechanism to track micro-cantilever movement, as well as an automated image capture and analysis system (Fig. 1).⁵⁾ By sensing an extremely frail interatomic connection between the specimen's surface and the probe tip, AFM examines the surface architecture and characteristics of the sample.⁵⁾ The anterior portion of the microcantilever, which is very sensitive to weak forces, whereas the cantilever's other end is fixed and is housed in the probe, is pulled close to the sample.²⁸⁾ Once this is done, there is a faint force involving the probe's tip and the atoms on the surface of the sample that may be either attractive or repulsive. The microcantilever's distortion or its state of motion are both affected by the strength of this force.⁵⁾ The end user can receive surface structure knowledge with nanoscale resolution by scanning the sample, which uses sensors to identify these modifications and gather force distribution data.⁵⁾ The X, Y, and Z axis of the AFM scanner are movable. Although the vertical Z direction's normal range is only a few microns, the X and Y orientations' travel distances depend on the scanner. Rebuilding the orientation of the PCS element in the Z-direction as well as the X-Y axis at the same moment allows one to determine the structure of the region being scanned.⁵⁾ Hertz's theory uses a linear fitting approach to calculate Young's modulus measurement for samples like tissues and cells, with a smaller value suggesting a specimen whose structure is more prone to deformation. The measured force between the tip and the specimen is reflected in the force-distance curve (Fig. 2a & Fig. 2b) that AFM measures. Force-time curves can also be employed to describe a substance's viscoelastic qualities in conjunction with force-distance curves.⁶⁾ This involves determining how much a specimen deforms over a period while being subjected to a constant load [creep response, Fig. 3a] or how much stress diminishes through time while being subjected to a steady deformation [stress relaxation response, Fig. 3b).^{6,13)}

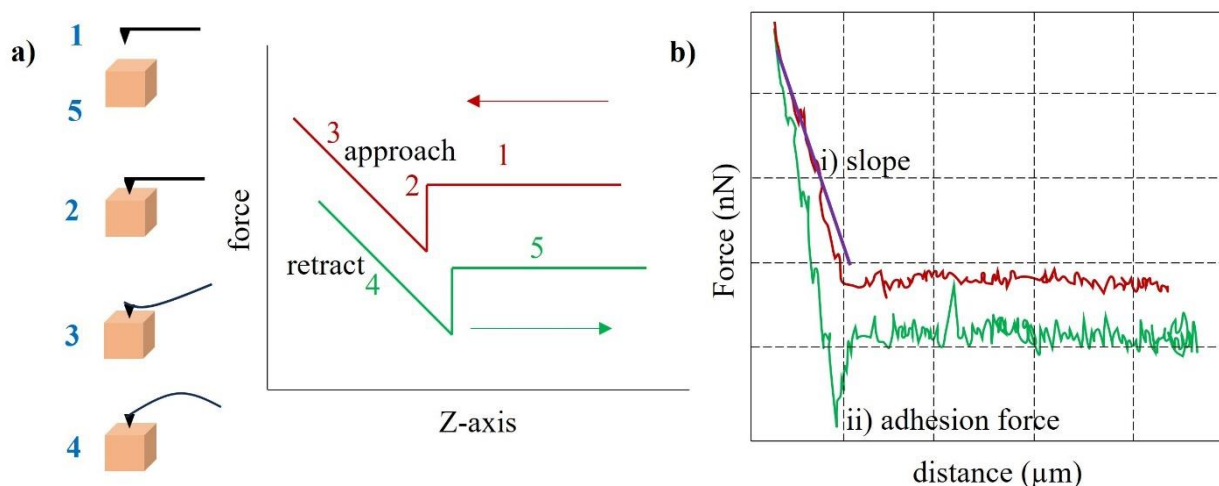


Fig. 2. Force-distance curve. a) approach (maroon) and retraction (green) of the AFM probe from the sample. The tip is distant from the sample surface [1], in contact with the sample [2]. During retraction [3], adhesive events may occur due to unspecific [4] or specific [5] interactions between the tip and the sample. b) The slope is fitted with a linear fit i) adhesion is measured as a single value and ii) refers to adhesion force.

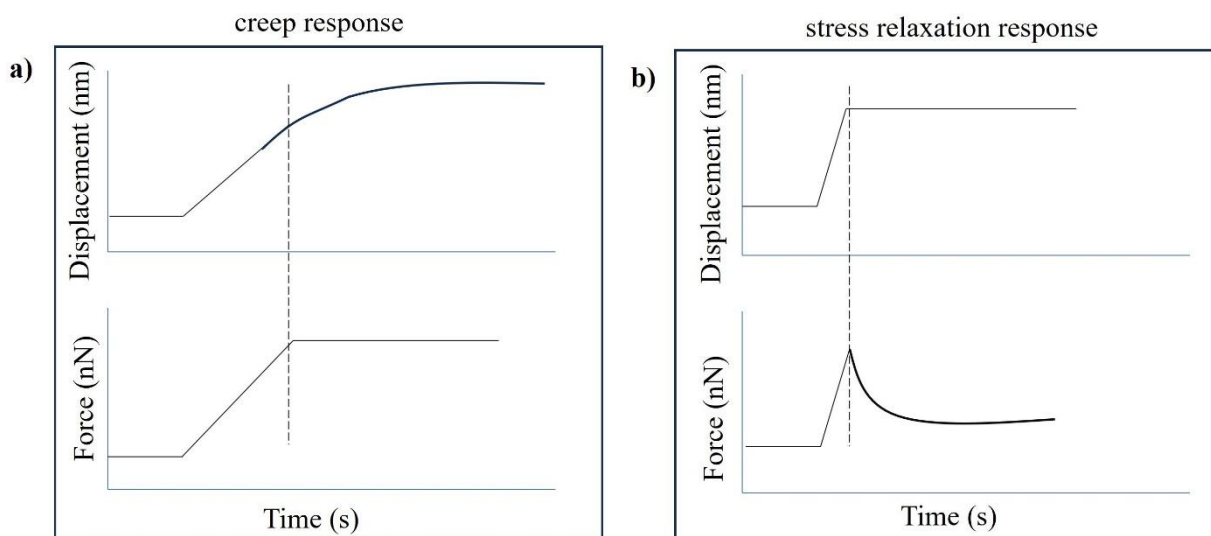


Fig. 3. a) force-time and b) displacement-time curves to characterize elastic or viscoelastic properties of the sample.

Force-time curves can be used to distinguish materials depending on their distinct viscoelastic characteristics.

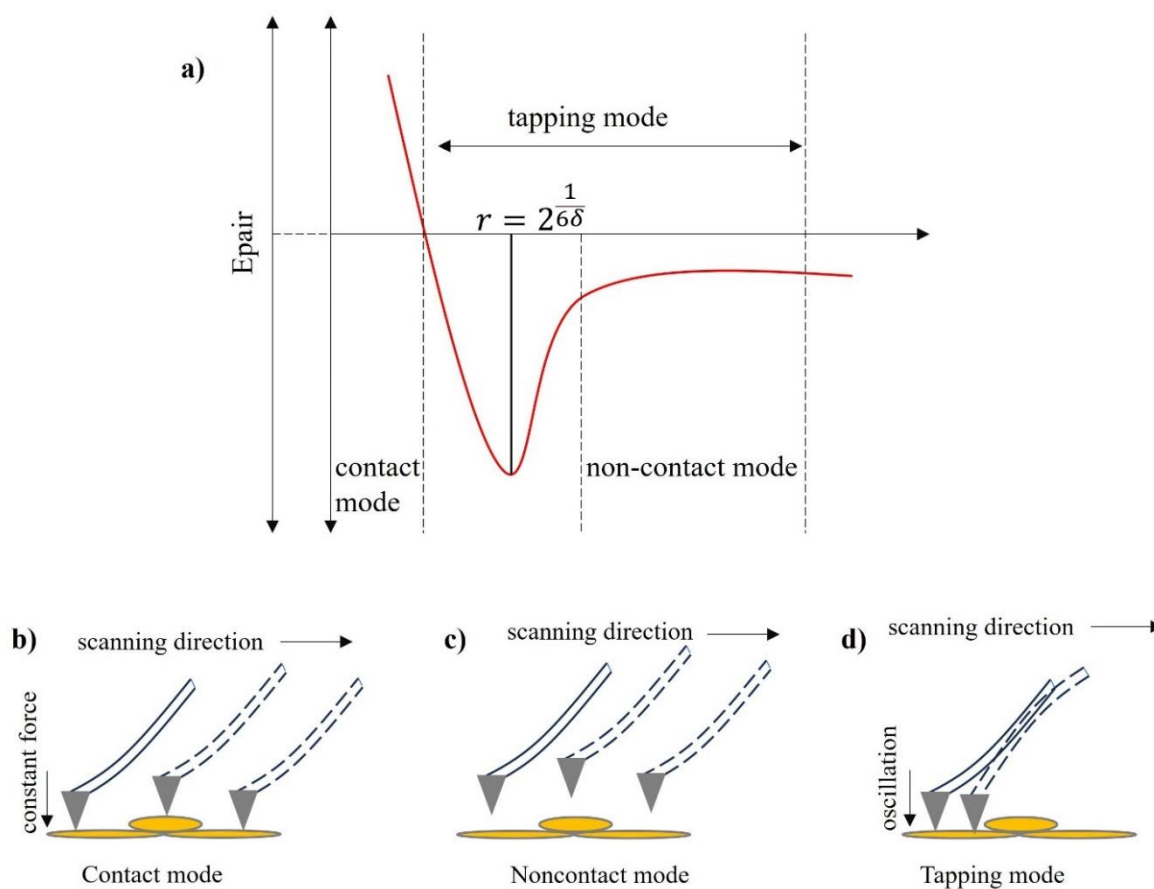


Fig. 4. a) relationship between interatomic force and interval, b) contact mode AFM operation, c) noncontact mode AFM operation, and d) tapping mode AFM operation.

The attraction-repulsion interactions among atoms serve as the foundation for the AFM visualization concept and mechanical characteristic detection.⁵⁾ If they are far enough apart from one another, the atoms at the probe's tip and the ones above the surface of the material become susceptible to an attractive attraction; whereas if they are close together, they are susceptible to a repulsive force (Fig. 4a). The contact (Fig. 4b), tapping (Fig. 4c), and non-contact modes (Fig. 4d) are the three fundamental imaging modalities of AFM.⁵⁾ During contact mode, the AFM probe retains a minimal amount of force and adheres to the sample surface. By detecting the atomic affinity between the probe and the specimen in non-contact mode, the surface profile of the specimen is generated.⁵⁾ The tapping mode enables the probe's micro-cantilever to oscillate near the resonance pitch, where it intermittently comes in contact with the specimen.⁵⁾ By adjusting the micro-cantilever's amplitude or deflection whenever the probe adheres to the sample, the force between both probe and the specimen can be kept steady.⁵⁾ Especially for the surface structure observations of biological specimens, tapping mode efficiently removes the impact of the lateral force and minimizes the force induced by the adsorption level, leading to excellent image resolution.⁵⁾

It is anticipated that employing AFM to analyze individual cancer cells will have two benefits. One way to diagnose cancer in its infancy is to look for alterations and variations in individual cells. By distinguishing between cancerous and non-cancerous cells, tumors can be detected and treated promptly.²⁹⁾ On the flip side, it makes it possible to investigate the composition and functioning of cancer cells as well as the mechanisms that contribute to their growth and division, cell-to-cell communication, and the impact of anti-cancer medications, among other things. The conclusions of these investigations could help scientists find ways to stop the growth of cancer cells and create anti-cancer medications.³⁰⁻³³⁾

2.1. Contact mechanics model. To generate force-distance profiles and calculate the Young's modulus of biological specimens, contact mechanics models based on Hertz (Equation 1) or Sneddon (Equation 2) are frequently utilized.⁶⁾ In contrast to the Sneddon model (spherical indenters), the Hertz model generally addresses conical indenters.⁶⁾

$$F(\text{Hertz}) = \frac{4}{3} \frac{E}{(1 - \nu^2)} R^{\frac{1}{2}} \delta^{\frac{3}{2}} [1]$$

$$F(\text{Sneddon}) = \frac{2}{\pi} \frac{E}{(1 - \nu^2)} \tan(\alpha) \delta^2 [2]$$

For blunted pyramidal tips, the Hertz-Sneddon model (Equation 3) is commonly utilized.

$$F(\text{Hertz} - \text{Sneddon}) = \frac{E}{(1 - \nu^2)} \frac{\tan(\alpha)}{\sqrt{2}} \delta^2 [3]$$

[F – applied load; E – Young's modulus; R – tip radius; ν - Poisson' ratio; δ - indentation depth; and α – cone half angle]

Investigators have utilized the Hertz and Sneddon contact mechanic models to assess the rigidity of a variety of tissue specimens, notably the developing cerebral cortex,³⁴⁾ pulmonary arteries,³⁵⁾ lung,³⁶⁾ rodent heart and pancreas,³⁷⁾ and blood vessels.³⁸⁾ Even though they are widely used, they do have some

shortcomings. The specimen must be isotropic, homogenous, elastic in nature, and not subject to significant distortions to be subjected to a Hertzian assessment.^{39,40)} In reality, biological tissues represent viscoelastic, heterogeneous, and anisotropic substances.⁴¹⁾ Therefore, it is impossible to reliably generate universal tissue biomechanical characteristics from just one regional assessment. Rather, a mechanical atlas of the respective tissue must be created by taking numerous local measurements across various sections of the complete tissue specimen.^{35,39,42)} In addition, it ought to be stressed that data gathering is limited to the specimen's surface, especially tissue specimens that are only a few microns deep. This is because for indentation levels greater than 10% of the thickness of a tissue, a Hertzian assessment is not appropriate. Additionally, it is preferable to determine a mean elastic modulus since the elastic modulus at one location frequently fluctuates throughout the axis of indentation.⁴¹⁻⁴⁴⁾ Therefore, if employing the Hertzian model to calculate the mean elastic modulus of their specimens, investigators ought to disclose the working indentation depths in addition to limiting the viscoelastic properties of their tissue specimens.^{41,43)}

2.2. Additional AFM imaging modes. Beyond the three primary modes (non-contact, tapping and contact modes), there are a variety of hybrid modes in which there are several types of tip-sample interactions. These include chemical force microscopy (CFM), AFM Infrared Spectroscopy (AFM-IR), force modulation mode, and contact resonance (c-resonance) mode. The contact resonance mode is a hybrid of the contact and the dynamic modes, in which the cantilever's resonance frequency is stimulated while it remains in touch with the sample. Using the more sophisticated AFM-IR mode as an example, this method combines an AFM with a laser source to characterize the material's photothermal absorption.⁴⁵⁾ AFM-IR integrates non-contact Photo-induced Force Microscopy (PiFM)⁴⁶⁾ and contact-mode Photo-thermal induced resonance (c-PTIR)⁴⁷⁾. A modified form of PTIR, which can be used in contact-resonance mode⁴⁸⁾ or tapping mode⁴⁹⁾, employs a pulsed laser close to the cantilever's resonance called resonance enhanced PTIR. In PiFM operation, the laser pulse frequency and the AFM cantilever piezo resonance excitation frequency can operate at the first cantilever resonance or, in a mode known as sideband bimodal detection mode, which is somewhat akin to multifrequency operation, they can cause deflection oscillation at both the first and second resonance. Consequently, AFM-IR can be considered as a sophisticated hybrid mode that combines dynamic and contact modes. One other hybrid mode that is worth mentioning is chemical force microscopy.⁴⁵⁾ Chemically active materials can be used to functionalize the cantilever's tip. It is a hybrid imaging mode because of the variety of interactions that might occur involving the tip and the sample. Similar methods, such as single-cell force spectroscopy, single-molecule force spectroscopy (SMFS), and single-cell force spectroscopy (SCFS), have been used in biomedical applications to investigate interactions between cells or molecules.⁴⁵⁾ Surface potential is measured using a technique called Kelvin Probe Force Microscopy (KPFM). This mode uses tapping mode to first make an imaging of the topography, then it uses the measured topography to create an "interleaved" repeating scan to identify the surface potential and subtract contribution from the topography.⁴⁵⁾ Both electrostatic force microscopy (EFM) and magnetic force microscopy (MFM) can be used in non-contact mode to measure electrostatic or magnetic force rather

than surface potential.⁴⁵⁾ The cantilever tip can be used to improve the localized electromagnetic field augmentation that contributes to increasing spatial resolution, in addition to its potential use for measurement. The scattering-type Scanning Near-field Optical Microscopy (s-SNOM) mode can be enabled by extracting a target signal with a vibration signature for spectroscopic purposes when paired with cantilever resonance excitation.⁴⁵⁾

To guarantee optimal imaging performance, it is crucial to choose the appropriate AFM modes of operation. Since biological samples are frequently brittle and soft, the fundamental AFM contact mode imaging technique may cause sample deformation by creating friction between the sample and the probe tip as it scans. Since soft biomedical samples are more likely to be destroyed and result in severe imaging aberrations, this is generally a more serious issue.⁵⁰⁾ For these kinds of applications, tapping mode that includes sporadic contact between the probe tip and sample is recommended. Maintaining the vitality of biomedical samples also requires careful control of the imaging environment. The native setting for the samples in many AFM investigations is a buffered solution. One possible application for the sample chamber that contains the fluid, sample, and cantilever probe is a fluid cell with liquid circulation. Functions for temperature control, fluid circulation, and carbon dioxide concentration adjustment may also be incorporated for more sensitive samples.⁵⁰⁾ Because of the medium's fluctuating refraction index, optical beam deflection alignment can become more complex even in transparent liquids. A tuning-fork based AFM can perform imaging in opaque liquid environments without the need for transparency, but it has a very high stiffness that is not good for biological specimens.⁵⁰⁾ Coated AFM probes with integrated active elements, like an electrothermal actuator and a piezoresistive deflection sensor, have been created for imaging applications to reduce stiffness.⁵¹⁾ The sample's optical microscope image is frequently crucial for biological applications since it aids in identifying the area of interest. AFM can be used in conjunction with fluorescent and confocal microscopy for advanced applications to create correlative microscopy, which compares pictures taken by the two devices. To achieve an improved fit with the optical images, it is noteworthy that a probe scan arrangement is frequently utilized for AFM in this situation.

2.3. Specimen preparation. During AFM testing, it is necessary to maintain the mechanical characteristics of the sample in addition to choosing an appropriate tip shape and contact mechanics' model. However, the mechanical properties of a sample are impacted by a variety of tissue handling and processing methods. To avoid tissues from migrating during data collection, for instance, they are frequently immobilized with adhesive glue.^{52,53)} Chemicals from the glue may diffuse into the tissue, affecting the specimen's mechanical characteristics even though there are techniques to prevent this.⁵²⁾ Another method by which tissues forfeit their mechanical integrity is through cryosectioning and chemical fixation. Chemical fixation is a popular technique that stops biochemical activities and cross-links proteins to maintain the tissue microarchitecture.⁵⁴⁾ Fixatives like formaldehyde and glutaraldehyde are used in this process.^{54,55)} Using a cryostat to cut the tissue into thin slices is a technique known as cryosectioning.⁵⁶⁾ As it would be challenging to cut tissues to precise proportions otherwise, this is desired.⁵⁷⁾

But through the creation of ice crystals and cell death, the freezing process frequently results in tissue damage and stiffness.⁵²⁾ These disadvantages mean that frozen and cryosectioned tissues are primarily utilized for imaging as opposed to mechanical characterization.^{52,58)} A further challenge is noise resulting from the cantilever tip's electrostatic interactions with the biological specimen and its environment.⁵⁹⁾ Several strategies have been developed to get around some of these issues. In a recent investigation, tiny slices of living brain tissue implanted in an agarose substrate were sliced by researchers using a vibratome. Because the agarose is unable to penetrate the tissue, this technique eliminates the requirement for chemical fixation, maintains the mechanical qualities of the tissue, and lessens the possibility that the slice may sustain physical damage.⁵⁸⁾ The AFM was repurposed for in vivo nanomechanical imaging and differentiation in rats.⁶⁰⁾ In this study, the aorta intima is exposed for simple cantilever tip accessibility using a three-component surgical base with a hollow dish.⁶⁰⁾ An advantage of this approach is that it mechanically characterizes vasculature in their native in vivo state. The resected tissue is occasionally kept in a suitable buffer or medium containing enzyme inhibitors immobilized on a glass slide, and subsequently evaluated shortly thereafter in research involving human cancer tissue biopsies.^{61,62)}

The advent of the FluidFM has made it an especially helpful tool for applications in biomedical research in liquid environments.⁶³⁾ An external microfluidic system can be used to apply suction pressure for the pick-and-place management of cells by employing a hollow cantilever containing an opening near the tip. Researchers may alter biological samples at the nanoscopic level with the help of these manipulation capabilities, which is far more accurate than using traditional needle-based micro-manipulation methods. For research on cellular adhesive contacts^{64,65)}, stress-dependent yeast cell mating⁶⁶⁾, and cellular detachment forces and energy, among other topics in cellular biophysics, this is an especially useful capability.⁶⁷⁾ Liquid can be precisely controlled and injected into or removed from the cell through the cantilever tip orifice if the probe tip permeates through the membrane to form small pores on the cell.⁶⁸⁻⁷¹⁾ In conjunction with optical and magnetic tweezers, fluidFM approaches have begun to gain popularity as tools for cell manipulation.

3. AFM in cancer research

For discussion purposes, the empirical studies reviewed were classified into two primary categories: Studies reviewed either focused on the performance or effect of anti-tumor drugs or studied the mechanical properties of cancer cells.

3.1. AFM, morphology, mechanical properties, viscoelasticity, and cancer research. Aquaporins are channels in the membrane that allow water and other minuscule, non-charged substances to move back and forth between cell membranes.^{72,73)} For maintaining the equilibrium of tissues, aquaporins are essential. More specifically, it has been shown that the peroxiporin subgroup regulates cellular redox balance and controls several physiological activities, including cell movement and growth. The emergence of oxidative illnesses associated with stress, such as cancer, is influenced by peroxiporin

dysregulation, which disrupts the delicately regulated redox equilibrium.⁷⁴⁾

Pancreatic ductal adenocarcinoma [PDA] is the most prevalent and fatal type of pancreatic cancer [PDA] while also being one of the most severe gastrointestinal cancers. Pancreatic cancer [PC] is the seventh most prevalent cancer globally and is the third-most common cause of mortality via oncologic causes in men and women in the European Union.⁷⁵⁾ Following a dysfunctional approach on BxPC-3 cells, Silva et al. (2022) assessed the roles of AQP3 and AQP5 in a cell's biomechanical characteristics, adhesion between cells, and cell mobility.⁷⁶⁾ In PDA, AQP3 and AQP5 have elevated levels and are important for cell movement, growth, and motility.⁷⁶⁾ Compared to control cells, the investigators discovered substantial morphological variations caused by AQP5 silencing, including a decline in cell area and volume, an upsurge in cell length, and an elevated level of surface abrasion.⁷⁶⁾ Contrarily, AQP3 suppression appeared to affect only the volume of cells. Cells with AQP5 silenced proved to be softer than cells used as controls, whereas cells with solely silenced AQP3 showed no discernible changes.⁷⁶⁾ As a matter of fact, the viscoelastic and morphological alterations demonstrated through the study depended heavily on AQP5 and were nearly devoid of AQP3, showing that AQP5 is crucial in regulating these cell features.⁷⁶⁾

Additionally, adhesion between cells was evaluated by AFM. Silencing of AQP3 and/or AQP5 was correlated with poor adhesion among cells, implying that AQPs are involved in cancer metastasis.⁷⁶⁾ Unexpectedly, in contrast to the initial phases of PDAC, AQP5 activity is essentially imperceptible in the later phases, supporting the findings and emphasizing the role of AQP5 in tumor malignancy. The critical role of AQP3 and AQP5 in the biophysical features of cell membranes is highlighted by these results, which may have implications for the environments in which tumors form.⁷⁶⁾

The most prevalent type of ovarian cancer and the leading factor in ovarian cancer-related mortality globally is high grade serous ovarian carcinoma [HGSOC].⁷⁷⁾ Morphological evaluation continues to serve as the primary screening method despite the adoption of homologous recombination deficiency screening in the clinical environment.⁷⁸⁻⁸⁰⁾ Since histological characteristics are believed to have predictive power in numerous reports, histological evaluation of H&E tissue slices under an optical microscope continues to be the primary and most helpful source of knowledge for pathologists due to the absence of viable molecular targets.⁸¹⁻⁸³⁾ Azzalini et al. (2021) examined the biomechanical attributes of HGSOCs growth patterns directly on conventional H&E tissue slices to investigate the diagnostic capacity of AFM and its prospective application in ovarian cancer pathology.⁸⁴⁾

The researchers identified a relationship concerning tumor rigidity and morphology by characterizing nanomechanically five distinct HGSOc morphological variations.⁸⁴⁾ Particularly, HGSOcs with micropapillary-like architecture exhibited comparatively low average rigidity levels, whereas HGSOcs with solid characteristics exhibited the highest average rigidity values and were therefore more comparable to healthy tissues (Fig. 5a and 5b).⁸⁴⁾ There has been a general consensus that cells with reduced rigidity have a better propensity for invasion than cells that possess greater rigidity.⁸⁵⁻⁸⁷⁾ Findings demonstrated that the micropapillary-like structure, which has undoubtedly the smallest Young's modulus relative to all other structures, might correspond to a specific invasive component in the broad range of HGSOcs.⁸⁴⁾ Findings indicated that individuals with stage III cancer had considerably firmer tumors than those with stage IV cancer, indicating a general trend among all HGSOcs forms to become less rigid and more aggressive as the illness worsens.⁸⁴⁾ Although the study only examined specimens with distinct morphological forms to measure tissue rigidity, multiple HGSOc forms sometimes appear in a single specimen.⁸⁴⁾ Consequently, additional investigations are required in specimens with numerous morphologies to confirm whether distinct biomechanical characteristics can be distinguished and aid in diagnosis.⁸⁴⁾

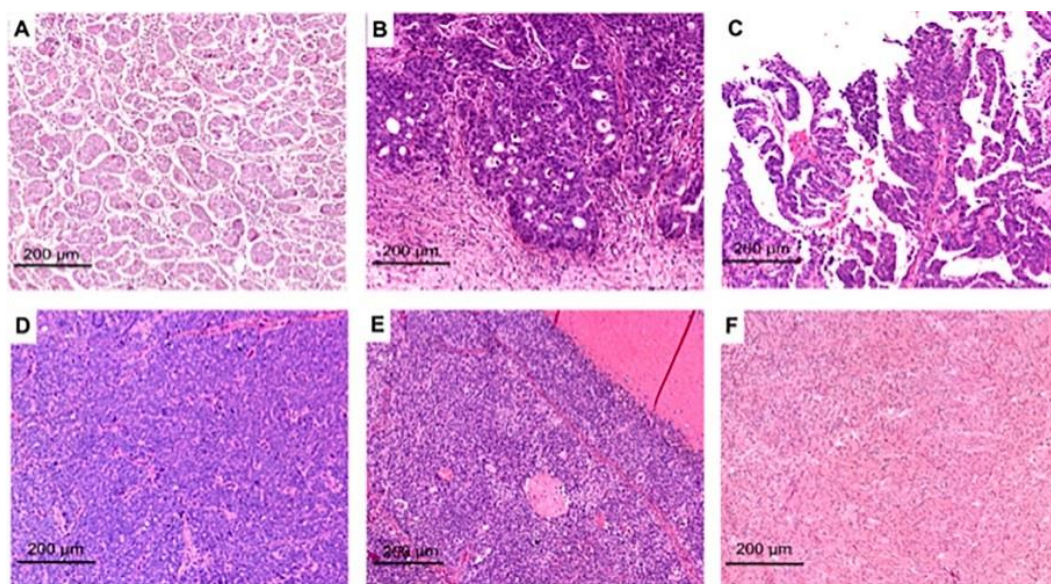


Fig. 5a. Representative optical microscope images of HGSOc patterns (A-E) and healthy peritoneal tissue (F). HGSOc patterns: micropapillary-like (A); endometrioid-like (B); papillary (C); solid (D); transitional-like (E); and healthy peritoneal fibrous tissue (F). Reproduced with permission from [Ref 57] @ ELSEVIER

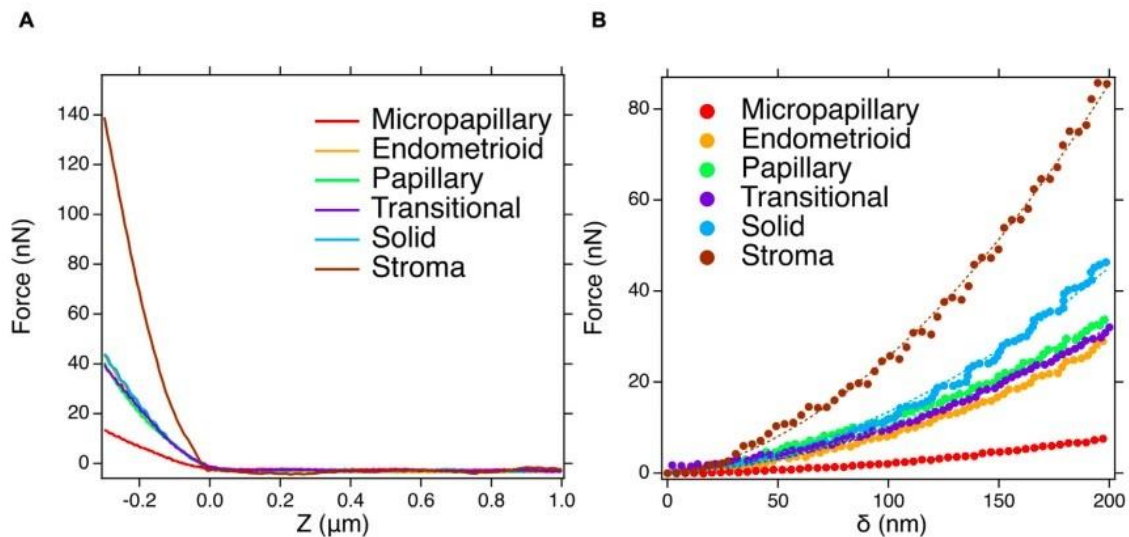


Fig. 5b. Representative curves of AFM force vs distance (A) and vs sample indentation (B) for the HSOGC patterns and healthy peritoneal tissue. In B dots show experimental force curves, and dashed lines are the curves fitted by the applied Hertz model. Reproduced with permission from [Ref 57] @ ELSEVIER

The second most fatal type of tumor for male patients, following lung cancer, is prostate cancer [PC], a frequent tumor of the male urinary system.^{88,89)} Because of the development of distant metastases, the majority of those diagnosed with extremely susceptible PC experience an unfavorable outcome as well as clinical treatment failure.^{90,91)} Tumor metastasis is mediated by a variety of causes. The extracellular matrix (ECM) happens to be one of them that is most strongly linked to tumor spread. Mechanical indicators like substrate rigidity, hydrostatic pressure, shear stresses, tension, and pressure are included in the ECM, which offers cells a favorable mechanical microenvironment.⁹²⁻⁹⁴⁾ Such mechanical elements are crucial in controlling both the growth of illness and routine cellular functions. It is unknown, nevertheless, how mechanical characteristics control how cells react to the ECM.

Tang et al. (2022) used polyacrylamide hydrogel platforms⁹⁵⁻⁹⁷⁾ to replicate the rigidity found in healthy and prostate tumor tissues by creating them with varying rigidity levels.⁹⁸⁾ By varying the substrate's rigidity, confocal microscopy, AFM, and other methods were utilized to examine how the viscoelastic characteristics of the cells changed throughout cell migration (Fig. 6).⁹⁸⁾ To improve PC-3 cells' capability to migrate across rigid substrates, the F-actin cytoskeleton was grouped into bundles, increasing its elasticity while decreasing the viscosity of the cells.⁹⁸⁾ In addition, the findings of the myosin-binding protein antagonist treatment revealed that variations in the arrangement of the F-actin cytoskeleton might have contributed to modifications in the mechanical characteristics of PC cells' reaction to the ECM.⁷¹⁽⁹⁸⁾ The presented research might present a novel strategy for exploring the migration process of PC tumor cells in addition to the cytoskeleton-mediated movement of PC cells, which can be beneficial to cancer therapeutic drug evaluation and advancement.⁹⁸⁾ This is because mechanical characteristics determined at the nanoscale may serve as a marker of cancer cell movement.⁹⁸⁾

The second-most deadly and third-most prevalent malignancy in the world today is colorectal cancer [CRC].^{99,100)} Insufficient cell transportation from the crypt, which is dependent on the APC protein,

contributes to the formation of CRC by causing a buildup of cells in the expanded zone of the intestinal crypt. By aggregating genetic changes, the quantity of these cells might exponentially rise, leading to the development of cancer.¹⁰¹⁾ To comprehend their involvement in the activation of oncogenes and tumor-suppressor gene suppression, several biochemical processes have been studied. Despite the growth of biochemistry studies, there remains more to be understood about the biophysical signals that activate the signaling networks important for mechanotransduction and cellular change. The understanding of these basic systems may aid in inhibiting oncogenic processes and the discovery of indicators that might be utilized to create more individualized therapy approaches.^{102,103)}

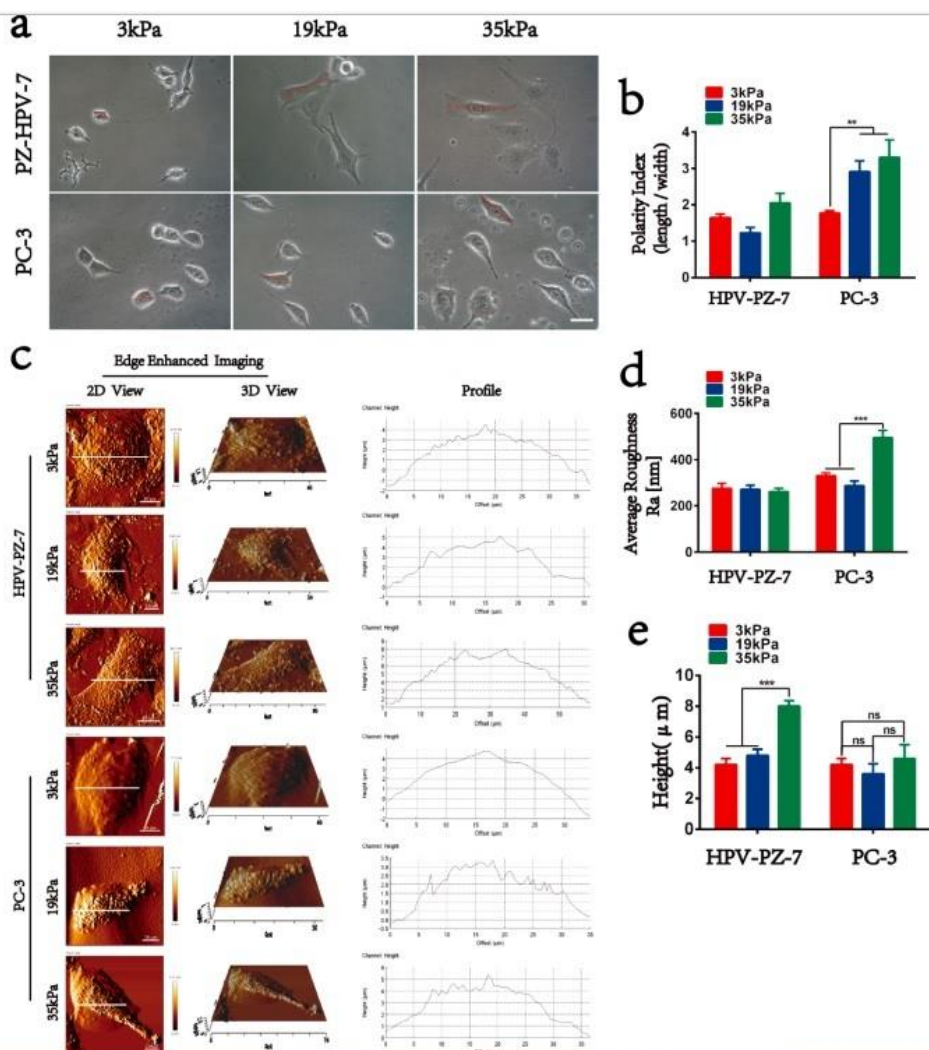


Fig. 6. Morphological analysis showed different characteristics in different stiffness. (a) Phase-contrast microscopy imaging of PZ-HPV-7 and PC-3 cells on substrates with different stiffness, scale bar = 10 μm . (b) Quantitative statistical graph of cell polarity index (length/width). (c) Atomic force microscopy imaging of HPV-PZ-7 and PC-3 cells on substrates with different stiffness. From left to right, the edge-enhanced images of cells are displayed, including two-dimensional and three-dimensional imaging and cell contour maps. (d) Quantitative statistics of the average surface roughness (Ra). (e) Quantification plot of cell height; “ns” means no difference, ** $P < 0.01$, *** $P < 0.001$. Reproduced with permission from [Ref 71] @ Beilstein

Brás et al. (2022) used static and dynamic AFM to examine the mechanical features of cells with CRC (HCT116, HCT15, and SW620).¹⁰⁴⁾ The dynamic method enables the measurement of pliability, viscosity, and mobility, while the static technique measures Young's modulus.¹⁰⁴⁾ The outcomes of confocal microscopy and migratory cell assays were correlated with the AFM results.¹⁰⁴⁾ SW620 metastatic cells had the highest Young's and storage moduli, a distinct cortical actin band with dispersed F-actin strands, little vinculin expression, lots of focal adhesions [FAK], and negligible filopodia growth, which could account for the reduced migratory tendency.¹⁰⁴⁾ HCT15 cells, in comparison, displayed lesser Young's and storage moduli, greater concentrations of cortical tubulin, reduced amounts of cortical F-actin and FAK, as well as greater filopodia production, which is likely what contributed to their increased migratory tendency.¹⁰⁴⁾ The strongest migratory behavior may be explained by HCT116 cells, which had Young's and storage moduli values that were comparable to those of the remaining cell lines, significant cortical F-actin expression, moderate levels of FAK, and profuse filopodia production.¹⁰⁴⁾

Modifications in the mechanical characteristics and makeup of TME are directly correlated with the advancement of cancer.¹⁰⁵⁾ The interaction of the various TME elements causes a desmoplastic reaction that occurs in numerous solid tumors, notably pancreatic cancer, which is primarily brought on by excessive production of collagen.¹⁰⁵⁾ Desmoplasia causes the tumor to harden, creates a significant obstacle to efficient drug administration, and is frequently linked to a bad prognosis.¹⁰⁵⁾ The discovery of innovative biomarkers for diagnosis and prediction can result from better knowledge of the underlying causes of desmoplasia and the determination of nanomechanical and collagen-based characteristics that define the condition of a specific tumor.¹⁰⁵⁾

In a recent work, Stylianou et al. (2023) described the distinctive nanomechanical characteristics of pancreatic tumors at different phases of advancement and normal pancreatic tissue.¹⁰⁶⁾ The elastic organization of regular pancreatic tissue possesses just a single peak, while pancreatic tumors exhibit unique lesser elasticity peaks and more elastic peaks, which correspond to tumor cell softening and desmoplasia, respectively.¹⁰⁶⁾ As expected, Young's modulus escalates as the cancer advances. In addition, the researchers demonstrate that the elevated elastic values are a result of evaluations taken in collagen-rich regions of the tissue using AFM in conjunction with CFM of picrosirius red-stained tissues. The prospect of creating new mechanobiomarkers is now open because of these studies.¹⁰⁶⁾

3.2. AFM, drugs, and cancer research. Alterations within the cytoskeletal design and subsequent alterations in cell rigidity, cell dry mass, and mobility might constitute significant supplementary consequences of numerous cytostatic medications because cellular bio-mechanical features, such as cell rigidity, are crucial for cell mobility.¹⁰⁷⁾ Raudenska et al. (2019) utilized AFM, quantitative visualization, and experiments to examine the effects of two commonly used chemotherapeutic medications, docetaxel, and cisplatin, upon an array of prostate cell lines with cancer.¹⁰⁸⁾

Docetaxel is produced from *Taxus baccata* needles. Docetaxel's main method of operation involves promoting and stabilizing microtubulin assembly, which obstructs microtubule activity.¹⁰⁸⁾ Suppression of cell growth, cell cycle arrest, and obstruction of mitotic proliferation are all consequences.¹⁰⁹⁾

Additionally, several studies suggest that cisplatin could influence the cytoskeleton in addition to DNA, which is the sole focus of the cell for this drug.^{110,111} These supplementary relationships might strengthen the inhibitory effect on proliferation and help cisplatin's cancer resistance effects, such as prevention of proliferation and movement.¹⁰⁸ In addition, zinc (II) ions, which are important for the cellular metabolism of the prostate gland and support an array of biological functions like apoptosis, the transmission of signals, and cell invasiveness,¹²⁻¹¹⁴ were tested for their impact on the biomechanical attributes of cells from prostate cancer. The investigation also examined whether or not the CAV1 gene, which is now believed to be related to cell stiffness via the modulation of actin remodeling and focal adhesions, affects the biomechanical characteristics of prostate cells with cancer.^{115,116}

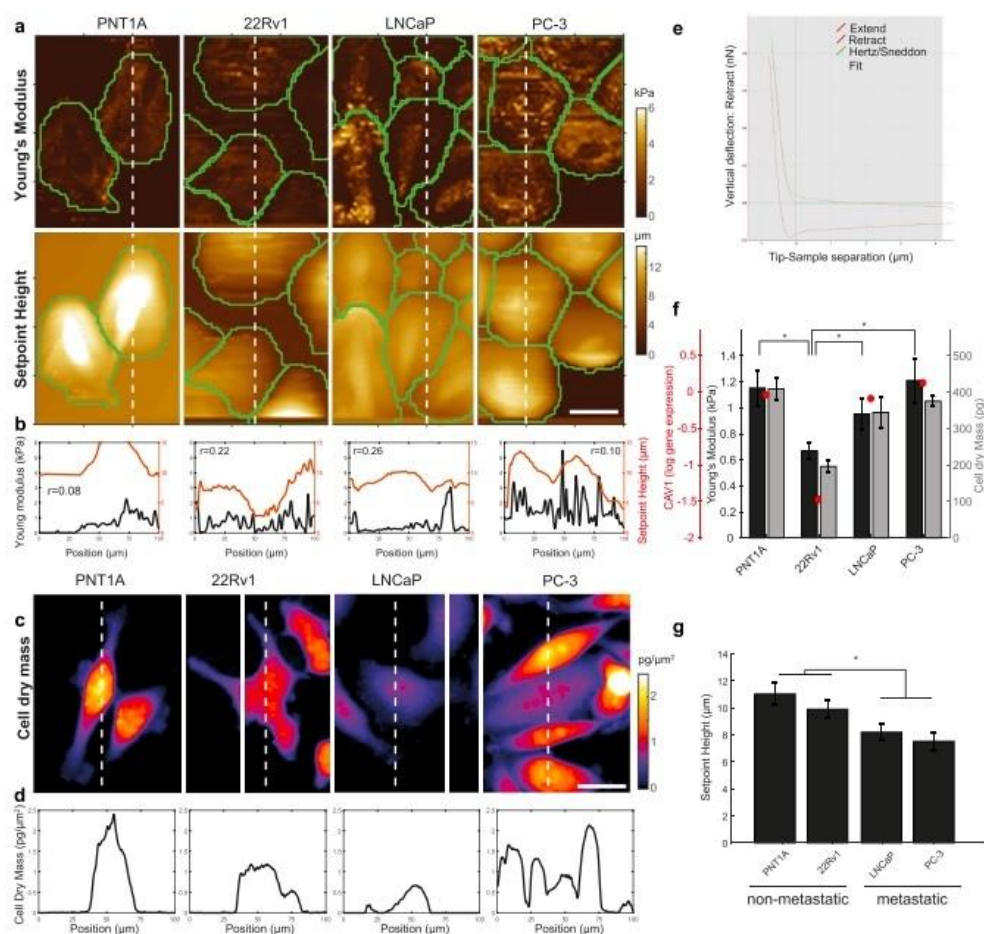


Fig. 7. Cell stiffness, cell dry mass and CAV1 expression of untreated prostate cancer cell lines. (a) Cell stiffness maps determined by indentation (Young's modulus) of prostatic cells (first row) and cell height (displayed as Setpoint Height, second row). (b) Profile of Setpoint Height/Young's modulus of red/blue lines shown in A together with pixel Pearson correlation values. (c) Cell dry mass. (d) Profile of cell dry mass in the corresponding cutting point (white line). (e) Hertz model fitting to a force curve obtained on PC-3 cells. (f) Values of Young's modulus, Cell dry mass, CAV1 gene expression for prostatic cells. Statistical significance shown for Young's modulus only. (g) Setpoint Height of cells. Significance between metastatic and nonmetastatic cells highlighted. Calibration bars for A and C represent 25 μm. Error bars denote standard errors. Reproduced with permission from [Ref 80] @ Nature

The features of tumor-transformed cells differ greatly from those of normal tissue-connected cells. Biomechanical parameters such as adhesion between cells and mechanical stiffness showed significant visible differences.¹¹⁷⁻¹²⁰ As a result, research on cell stiffness has revealed that malignant cells are typically less rigid than their healthier counterparts.¹²¹⁻¹²³ According to the study's findings, cancer cells obtained from the primary tumor region (22Rv1 cells) appeared significantly stiffer than cancer cells obtained from healthy PNT1A cells [prostatic tissue], but this did not prove the case for the cell types used to treat metastatic cancer [LNCaP and PC-3].¹⁰⁸ The findings also point to a potential involvement of CAV1 in the overall stiffness of prostate tumor cells and a favorable relationship between cell stiffness and dry mass in both treated and untreated cells.¹⁰⁸ The study's findings demonstrate that the cytoskeleton is crucial in the modification of cancer cells' biomechanical properties since docetaxel therapy, which stabilizes microtubules and inhibits their movements, significantly increases the cell's stiffness (Fig. 7).¹⁰⁸ This observation is well-supported by additional studies.^{124,125} Additionally, cisplatin therapy significantly increased the prostate cancer cells' cellular stiffness. In all studied cell types, a significant reduction in cell movement, spread, and colony formation was seen in cells that had endured the docetaxel and cisplatin therapies.¹⁰⁸

Physical forces can regulate cellular activity in eukaryotic cells via the cytoskeleton polymers.^{126,127} The ultimate mechanical functions, including cell mobility and segmentation, are affected by cytoskeletal dynamics.^{128,129} Its malfunction could lead to cellular death, instability of the chromosome, making it a frequent and desirable target for therapeutic development.¹³⁰ A strong technique for imaging with high resolution and mechanical characterization of single-cell research in approximately physiological settings. It can identify a range of forces between pico and nanoNewtons.^{131,132} The AFM approach offers a substitute for assessing drug-cell relations and can assist in understanding how medications influence how cells function.^{129,131}

It has been empirically shown that the natural chemical piperlongumine [PL], which originates from pepper species, exhibits anti-cancer effects on HeLa cells. In reaction to the existence of PL, Contessoto et al. (2021) mechanically characterized HeLa cells. Utilizing AFM and single-cell manipulation, evaluations were carried out on HeLa cells under various conditions during PL therapy and the associated controls.¹³³ The findings demonstrated that the step force "SF" is dependent on the drug's duration of action period; PL begins to affect HeLa cells within the initial six hours of therapy.¹³³ Furthermore, SF is susceptible to chemical concentration; HeLa cell tests using 5 to 10 μM of PL therapy show a rise in SF, with a fluctuation of about 10 pN. SF is susceptible to changes in the cytoskeleton in addition to action time and concentration.¹³³ Irrespective of substrate rigidity, HeLa cells in the presence of 10 μM of the PL enhance the tethering force in comparison to the control. Such an SF increase shows the possibility that HeLa cells' microtubules are the target of PL action.¹³³

Crohn's disease and ulcerative colitis are two examples of inflammatory bowel diseases "IBD", which are complex gastrointestinal disorders. Extended therapy with medications and possibly surgical treatments is required for individuals with IBD.¹³⁴ The therapeutic environment for IBD has been substantially altered by the introduction of infliximab. Nevertheless, despite its demonstrated

effectiveness in inducing and maintaining clinical recuperation, mounting data points to a possible link between unsuccessful therapy and insufficient medication plasma concentrations.¹³⁵⁾ While ELISA

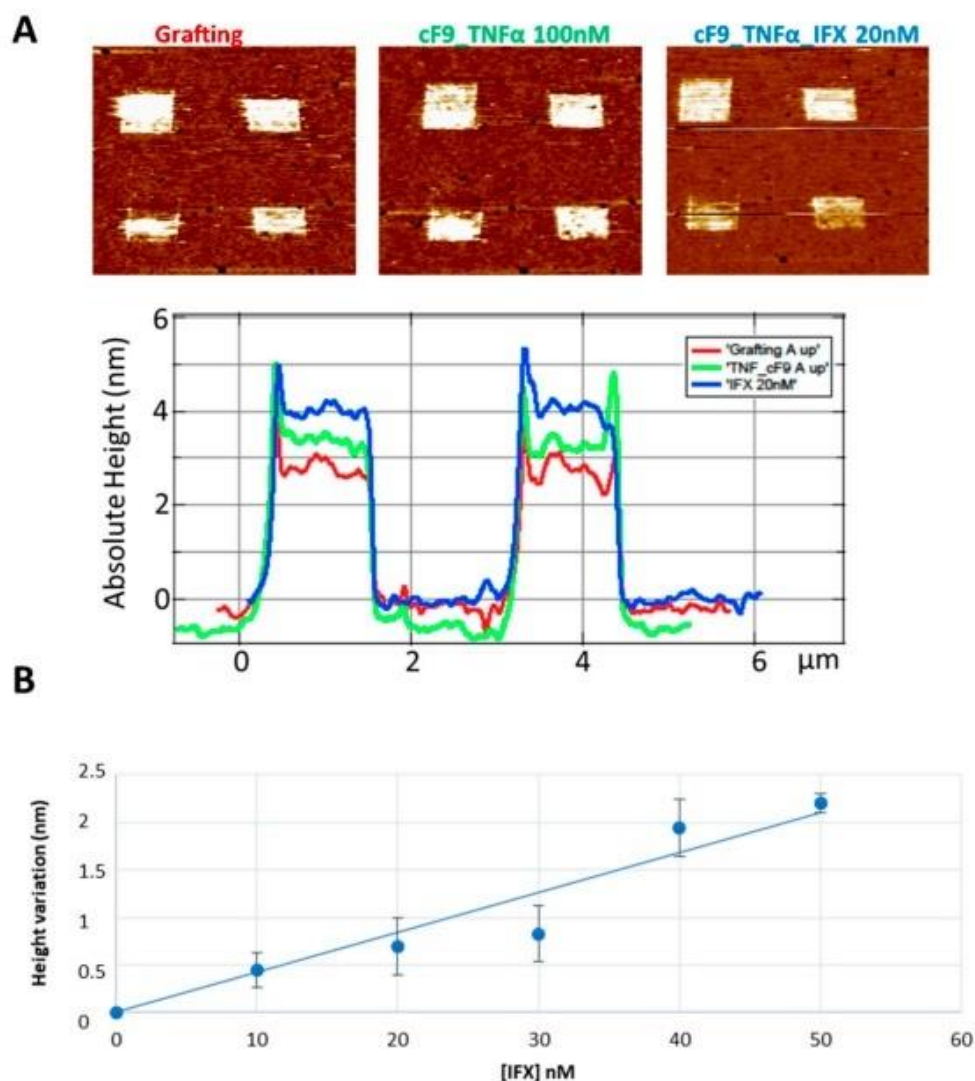


Fig. 8. a) an example of DNA nanostructures characterization by AFM topography: different DNA patches profiles with different height taken from AFM images (red line: ssDNA; green line: TNF-cF9 conjugate; blue line: infliximab (IFX) 20 nM); (B) the calibration line obtained in healthy donor sera spiked with IFX at different concentrations. Reproduced with permission from [Ref 110] @ MDPI

assays continue to serve as the test of choice for therapeutic drug monitoring, or "TDM," in clinical settings,¹³⁶⁻¹³⁸⁾ they can be costly, particularly when handling a small number of specimens. During the rapid assessment of medicines for TDM, the implementation of biological sensors built on several nanostructured substances has been proposed.

For determining the concentration of infliximab in specimens containing serum from healthy individuals and young individuals with IFD, Curci et al. (2022) employed an AFM-based nano assay.¹¹⁰⁽¹³⁹⁾ The experiment determined the height signal fluctuation of a gold surface that was nanostructured and covered in a self-assembled single layer of alkanethiols.¹³⁹⁾ A DNA-coupled

malignant necrosis agent that could recognize the medication was encased within the monolayer.¹³⁹⁾ The technique was first adjusted by evaluating established infliximab amounts in buffer, then proceeded to test young individuals with IBD after stimulating the same amounts of infliximab into the serum of healthy volunteers (Fig. 8). The prospective application of the AFM nano assay in TDM was demonstrated by the strong association between height fluctuation and drug concentration in the buffer medium across healthy and young IBD patients.¹³⁹⁾

Several tumors, including breast cancer and some sarcomas, become more rigid once they spread into healthy tissue, whereas the cancerous cells themselves become softer. The proper distribution of medications is significantly hampered by tumor rigidity, which also hinders the effectiveness of therapies.¹⁴⁰⁾ The regulation of a tumor's mechanical characteristics by focusing on the tumor microenvironment's "TME" components improves the transport of chemotherapy drugs and, as a result, the therapeutic result. Therefore, there exists an immediate demand for the creation of biomarkers that can quantify the mechanical properties of a specific cancer to establish tailored therapies or to track therapeutic approaches that focus on the TME.¹⁴⁰⁾

To combat fibrosarcoma and breast cancer in animal models, Stylianou et al. (2022) discovered that coupling tranilast with doxorubicin considerably lowers the Young's modulus and substantially improves chemotherapy efficiency.¹⁴⁰⁾ Most significantly, tranilast can lessen tumor rigidity by lowering the concentrations of extracellular substances, including collagen and hyaluronan.¹⁴⁰⁾ As a result, during the duration of clinical treatment, AFM can establish mechano-biomarkers that change along with changes in the tumor's mechanical properties.

4. High speed AFM imaging

Enhancing the speed of AFM imaging has long been a subject of research in the field. The probe-sample contact is used in the AFM scanning process to record a single pixel at a time. The creation of even a single image using conventional AFM imaging takes many minutes. However, biological processes can happen in milliseconds, necessitating higher frame rates for imaging. A skeletal myosin II power stroke, for instance, occurs within milliseconds, necessitating high-speed AFM (HSAFM).¹⁴¹⁾

The engineering difficulty of designing a HSAFM is substantial and necessitates the modification of numerous subsystems. Miniaturized cantilever probes that are nanofabricated have been created.¹⁴²⁻¹⁴⁴⁾

The cantilever responds to changes in the sample topography more quickly when its resonance frequency is high. The cantilever's stiffness (k) to mass (m) ratio is directly related to the square root of its first resonance frequency, ω . The cantilever's size should be decreased since it should maintain a small degree of rigidity to protect the delicate biological sample. It is also necessary to modify the deflection sensors for the shrunken probe, such as the optical beam deflection system's smaller laser spot.

Although ideal, high-speed imaging with a large scan area can be difficult, particularly for soft samples.

Small scan regions are usually employed in high-speed imaging because such samples require a minimal tip-sample contact force. Thankfully, it is possible to track the motion of microscopic target particles when the frame rate is high enough to outpace the rate of a dynamic process that needs to be photographed.¹⁴⁵⁾ For correlative examinations of biological samples, the HSAFM technique can also be used with other techniques such near-field fluorescence microscopy.¹⁴⁶⁾

It remains difficult to image the mechanics of live cells at high speeds with AFM, even after small cantilevers¹⁴⁷⁻¹⁴⁹⁾ and HSAFM were developed.¹⁵⁰⁻¹⁵⁵⁾ This is because most modern HSAFM setups lack the tools necessary for mechanical measurements, have a small scan range, and cannot do simultaneous optical microscopy. They also often lack environmental control.

In a recent study, HSAFM is used in conjunction with fluorescence and optical phase-contrast microscopy.¹⁵⁶⁾ With the use of tiny cantilevers, the system makes it possible to photograph living cells

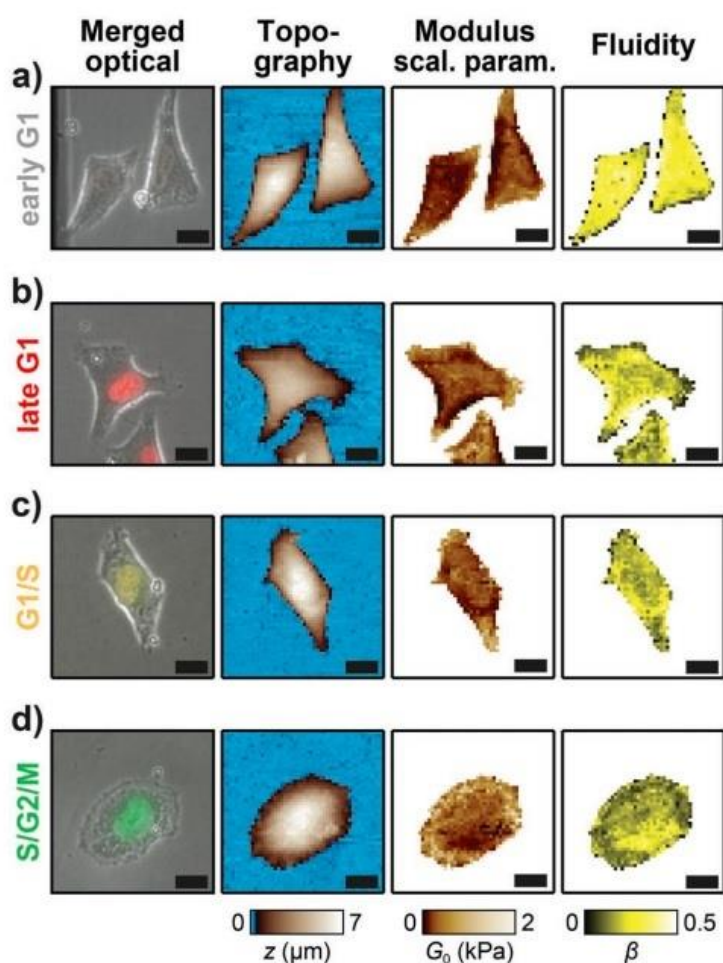


Fig. 9. Mapping of viscoelastic material properties of live WM938 cells in different cell cycle phases. a–d) Phase-contrast overlaid with fluorescence from optical microscopy, topography, modulus scaling parameter G_0 , and fluidity β from FCFM for cells in a) early G1 (colorless nuclei), b) late G1 (red), c) G1/S (orange), and d) S/G2/M (green) phase. Scale bars 20 μm , pixel resolution 50 \times 50, trigger force 1.3 nN, ramp size 2.5 μm , approach velocity 50 $\mu\text{m s}^{-1}$, image rate 4.2 min per frame. Topography images show the “true” (zero-force) height that was calculated from the contact point of the force curves. [Ref 156] @ Wiley

in typical cell culture dishes while controlling the CO₂ and temperature.¹⁵⁶⁾ Fast force mapping is carried out on living human platelets to showcase the setup's potential. Additionally, live cancer cells' optical phase-contrast and actin fluorescence images, as well as HSAFM images, are recorded simultaneously. Two cutting-edge AFM modes—force clamp force mapping [FCFM], and resonance compensating chirp mode [RCCM] for imaging viscoelastic sample properties are also compared.¹⁵⁶⁾ Additionally, the researchers assessed the cell volume, shape, and viscoelastic material properties of live cells as a function of their cell cycle status using a fluorescent cell cycle sensor equipped with melanoma cancer cell line. Across the cell cycle (G1 through the G1/S to the S/G2/M phases), the researchers were able to show that cell volume, area, and stiffness rise while fluidity decreases (Fig. 9).¹⁵⁶⁾ Findings suggest that when combined with optical microscopy, HSAFM with a wide scan range can offer fresh perspectives on cell mechanics in scenarios that are important to pathology or physiology.¹⁵⁶⁾

5. Hybrid AFM techniques

For many cancer patients, the cause of mortality is distal metastases. It follows that an understanding of the distinctions between primary and metastatic cancer cells is essential for both cancer diagnosis and treatment. Raman spectroscopy has demonstrated the ability to effectively discriminate between malignant and non-cancerous tissues, as well as between primary and metastatic cancer cells.¹⁵⁷⁾ One of the most significant advantages of Raman spectroscopy over AFM is its ability to determine a substance's chemical makeup.¹⁵⁸⁾ The application of AFM can be expanded by combining it with Raman spectroscopy [133]⁽¹⁵⁹⁾ to simultaneously assess the chemical composition of the substance and the amount of material present on the cell surface. The following recent studies have consistently demonstrated the advantage of combining AFM and Raman spectroscopy.

To create antiangiogenic medicines for use in clinical practice, it is essential to comprehend biological predictive markers and angiogenesis mechanisms. The biochemical makeup and mechanical topography around blood arteries in the tumor mass of human breast tissue were investigated by Kopec et al. (2018).¹⁶⁰⁾ Because of their great spectral and spatial resolution, as well as their sensitivity to minute chemical, structural, and topographical changes, integrated micro-Raman and AFM imaging are effective techniques for studying human tissue.¹⁶⁰⁾ The Raman spectra offers information on the collagen network, namely the determination of type III collagen fibrils, which is not readily accessible through other methods of imaging. The benefit of Raman spectroscopy is its ability to detect type III collagen fibrils that do not exhibit PAS staining and have a high percentage of carbohydrate polymers.¹⁶⁰⁾ The findings showed that breast cancer-specific biochemical and mechanical changes in the tumor mass surrounding blood vessels in both malignant and healthy human breast tissues could be simultaneously identified using Raman imaging and AFM. High-resolution Raman and AFM maps demonstrate that changes in the biochemical makeup of the tumor microenvironment, which is made

up of both cellular and non-cellular compartments, are the cause of matrix stiffening during the evolution of tumors.¹⁶⁰⁾ Significant changes in the chemical composition and structural architecture around the blood vessel, together with a notable expansion in the collagen-fibroblast-glycocalyx network, are suggested by the results. Raman-based techniques can be used to readily monitor the increased lactic acid and glycogen activities of cancer tissue in oncogenically altered cells.¹⁶⁰⁾

AFM imaging, which maps the chemical distribution of constituents, cell stiffness, and adhesion, in conjunction with Raman microscopy imaging, has been shown to be an exciting substitute for quantitative assessments of metabolic dysfunction in living cancer cells.¹⁶¹⁾ Raman imaging in conjunction with AFM and fluorescence microscopy was used to provide biochemical mapping and nanomechanical properties (topography, stiffness, and adhesion) of the human breast and brain for normal and cancerous tissues as well as the cell culture line U87 MG of glioblastoma.¹⁶¹⁾ Thorough examination of in situ breast ductal carcinoma, astrocytoma brain tissues, and glioblastoma U87 MG cells revealed that Raman scattering produces images with the same level of accuracy as the histopathology hematoxylin and eosin stain utilized in clinical settings, plus the added benefit of biochemical information. Correlating the mechanical characteristics of cells with their biochemical makeup is possible through the integration of AFM maps and Raman images.¹⁶¹⁾

Biologically active substances known as statins function as HMG-CoA reductase inhibitors, which inhibit the enzyme that catalyzes the conversion of 3-hydroxy-3-methyl-glutaryl-CoA [HMG-CoA] to mevalonic acid. Statins reduce systemic cholesterol concentrations by inhibiting the manufacture of endogenous cholesterol through their action on this enzyme.¹⁶²⁾ However, research conducted both in vivo and in vitro has confirmed that statins have cytotoxic and cytostatic effects on a variety of cancer cell types, including colon cancer. In a recent study, the effects of mevastatin on CaCo-2 malignant colon cells are examined using Raman spectroscopy and imaging, and their biochemistry is contrasted with that of CCD-18Co normal colon cells.¹⁶²⁾ Mevastatin's impact on the biochemical makeup of cancerous human colon cells has been proven through analysis of the vibrational characteristics of three types of colon cells: normal cells (CCD-18Co), cancerous cells (CaCo-2), and cancerous cells (CaCo-2 treated with varying doses and incubation periods).¹⁶²⁾ The nanomechanical characteristics of healthy CCD-18Co and malignant CaCo-2 human colon cells were characterized using AFM both with and without mevastatin treatment. The examination of force-distance curves revealed that malignant cells have a lower Young's modulus value than healthy cells. Young's modulus increased by almost 80% upon the addition of mevastatin, indicating that mevastatin affects the arrangement of the cellular cytoskeleton. The idea of using nanomechanical parameters to track changes typical for tumor development and anti-tumor treatment is justified by the application of AFM to describe elastic properties of normal and malignant cell lines.¹⁶²⁾

To investigate the mechanical characteristics of individual cancer cells, AFM can be used in conjunction with a confocal laser scanning microscope (CLSM).¹⁶³⁾ Indentation points and imaging of subcellular components are intimately correlated when AFM and CLSM are used together.¹⁶⁴⁾ Alpha-enolase (ENO1) is a multifunctional protein that has two functions: it is a fibrinogen receptor that stimulates

the spread of cancer and one of the enzymes engaged in glycolysis.^{165,166)} The use of AFM and CLSM in tandem demonstrated that ENO1 gene suppression coarsened the cellular morphology of pancreatic cancer, impairing the adhesion between the cancer cells and the stroma, ultimately leading to the invasion and metastasis of the cancer cells.¹⁶⁷⁾

5. Conclusion and Future Outlook

Variations in the mechanical characteristics of tissues and cells during stages of cancer progression may offer significant insights for facilitating the development of innovative treatment approaches along with improving the identification and classification of different types of cancer. AFM has gained popularity as a means of assessing cell and tissue mechanics because of its capacity to examine biological materials under physiologically realistic circumstances.^{168,169)} Numerous studies are currently using AFM to produce nanomechanical signatures of different malignant and non-malignant tissues, realizing the significance of whole-tissue mechanics in the evolution of cancer (Table 1). The creation of Young's modulus maps of tissue samples using the Hertzian, Sneddon, or a comparable contact mechanics model forms the basis for the majority of the nanomechanical fingerprints discussed in this paper. Consequently, it is now recognized that a variety of tumor and tumor-bearing tissues have a unique mechanical fingerprint in comparison to healthy tissue. AFM has grown in popularity as a method for assessing cell and tissue mechanics,¹⁷⁰⁾ evolving from its earliest visualization techniques (contact and tapping modes) and force curve-based mechanical assessment methods to contemporary rapid imaging techniques such as fast-scan mode¹⁷¹⁾ and high-resolution mechanical assessment using peak force mode.^{172,173)} Many studies have already begun to employ AFM to establish nanomechanical fingerprints of different cancerous and non-malignant tissues due to its capacity to analyze biological specimens in physiologically appropriate settings. The majority of the nanomechanical fingerprints discussed in this overview are primarily based on the construction of tissue specimens with Young's modulus correlates utilizing the Hertzian or Hertz-Sneddon contact mechanics model. Before the use of AFM technology is capable of being effectively implemented in the real world, there remain a lot of challenges that need to be addressed.

Another necessity is the uniformity of AFM measurements. When AFM is utilized for assessing a cell's mechanical characteristics, the Young's modulus serves as a parameter that is frequently calculated. However, this parameter depends on the experimental scenarios,¹⁷⁴⁻¹⁷⁷⁾ equipment settings,¹⁷⁸⁾ cell state,¹⁷⁹⁾ data evaluation,¹⁸⁰⁾ and so forth. It is challenging for scholars to uphold similar experimental settings, and outcomes from numerous experiments are only comparable if the circumstances are completely consistent.

A biological material's mechanical integrity is not just determined based on its elastic characteristics. In fact, scientists are just starting to look at the significance of viscous forces when handling tissue samples. By considering such viscous forces, researchers can find new biomarkers and create a more thorough mechanical characterization of cancerous tissue. Only a couple of the papers that were

analyzed looked at the viscoelastic qualities of cancer cells. Consequently, for optimal screening and therapy in healthcare facilities, future research should concentrate on describing the viscoelastic properties of tissues. This will help us better comprehend the mechanopathology of tumor tissues. Hence, the methodology for measurement as well as specimen preparation must be regulated to be able to render the assessment outcomes from different study teams consistent.

AFM's responsiveness and stability at different temperatures currently place constraints on how accurately it can describe biological systems. The recently developed ultra-stable AFM can offer sub-pico force accuracy while offering great stability with very little lateral drift.^{181,182} AFM technique will become more crucial to cancer studies and diagnostics as it is continuously developed and improved.

Clinical research may find the automated process of AFM analysis of information to be of great value. Yet, there isn't a standardized method for using this approach to investigate tissue samples.¹⁸³ While thinking about clinical transformation, attempts must be made to regulate the utilization of AFM to produce reproducible and precise findings.¹⁸³ This involves employing the same tip characteristics, becoming in tune with specimen handling and treatment, implementing consistent operating variables across different specimens, implementing appropriate simulations for mechanical evaluation, and contrasting outcomes with other conventional material analysis methods for verification.¹⁸³

The most challenging component of the evaluation is figuring out how much each element corresponds to the mechanical characteristics of tumor tissue. Additionally, tumor tissue has a greater level of heterogeneity, with variations appearing in both the same tissue and in several tumor tissues.¹²³⁽¹⁸³⁾ Because of this, it is necessary to separate distinct parts of the tissue for contrast detection because tumor tissues in various areas may have varied mechanical attributes. As a result, it is necessary to regulate the handling of samples and AFM evaluations as well as identify the relative values that distinguish cancer cells from healthy cells.

It is necessary to enhance both the temporal resolution and the efficiency of utilization. Currently, AFM cell measurement is mostly carried out manually. This includes offline evaluation of experimental data, manually selecting parameters to create cell force curves, and manually guiding the probes to target cells. As a result, the experimental efficiency is relatively low, and measuring a cell takes several minutes.¹⁸⁴ Specifically, measuring a large number of cells is required to generate statistically meaningful conclusions. This leads to a high burden and restricts the real-world use of AFM at the single cell level. As a result, increasing AFM's automation level will contribute to increasing measurement efficiency. Furthermore, the cell's response time to the environment is roughly 1 ms, which is a lot faster than the mechanical mapping time of AFM, which is roughly 10 min.¹⁸⁵ As a result, it is challenging to track changes in a cell's mechanical characteristics in real time. Despite being commercialized,¹⁸⁶ HS-AFM is appropriate for imaging flat and rigid small-size samples, like molecules bound to a substrate.¹⁸⁷ Moreover, real-time studies examining modifications to the fluctuating mechanical characteristics of cells^{188,189} will benefit from accelerating the pace of AFM detection. Imaging of the cells of mammals is another application for high-speed AFM.¹⁹⁰ Compared to the time it takes for cells to respond to external stimuli, the imaging duration is often much longer (~

5 s).¹⁹⁰⁾

As advanced computational methods gradually acquire popularity in AFM research, data processing errors might become less common and data analysis times might be shortened. Interestingly, to interpret AFM nanoindentation data more correctly, machine learning techniques¹⁹¹⁻¹⁹⁴⁾ and finite and inverse finite element models¹⁹⁵⁻¹⁹⁷⁾ have been developed and subsequently put into practice. For instance, automated neural network analysis that assesses force–distance curves allowed to distinguish between cancerous and healthy tissues.¹⁹⁴⁾ In healthcare settings, the computerization of AFM data evaluation might prove to be highly beneficial. Nevertheless, there isn't a standardized method for using this technique to investigate tissue specimens. Before thinking about clinical translation, efforts should be made to harmonize the utilization of AFM to get reproducible and accurate results. Using the same tip properties, handling, and treating samples consistently, applying suitable models for mechanical characterization, applying the same operating parameters across specimens (e.g., indentation depth, indentation rates, scanning area, force), and verifying results by comparing them with other traditional material characterization techniques are some examples of this.¹⁹⁸⁾ Optimization trials may be required to determine the optimal settings for a given sample type, as these factors may differ amongst different types of samples. The foundation for determining the best practices for the AFM-based substance and biomechanical assessment of malignant tissues is laid by studies like the ones included in this review. Furthermore, since generalized methods are not constrained by the same limitations as the Hertzian and Sneddon models, they would be more appropriate for a precise and consistent mechanical characterization of tissue samples. Examples of these approaches include those reported in.^{199,200)}

The electromagnetic spectrum, which includes information on material properties, cannot be directly sensed by AFM in its natural state (such as light color). Color can be understood as the sample material's absorption/reflection spectrum over a broad wavelength range at the microscopic level.⁴⁵⁾ Since such a spectrum is not naturally available in a traditional AFM setup, two electromagnetic wave emission and detection sources are usually needed for the measurement of such spectrum. As a result, meeting the demanding requirements in biomedical research with traditional AFMs in their most basic form is difficult.⁴⁵⁾ Thanks to appropriate AFM system modification and technique combination, the AFM technology has fortunately developed quickly to acquire novel possibilities and overcome current constraints based on experimental needs.⁴⁵⁾

Considering the results of the empirical studies reviewed, AFM has the potential to be an effective technique in cancer studies with clinically feasible applications, such as the discovery and confirmation of clinical biomarkers.

Acknowledgements

The authors would like to thank the professors who provided helpful criticism and feedback.

References

1. Pérez-Domínguez S, Kulkarni SG, Rianna C, and Radmacher M. Atomic force microscopy for cell mechanics and diseases.(2020) *Neuroforum*. 26,101-9.
2. Wei F, Wu Y, Tang L, Xiong F, Guo C, Li X, Zhou M, Xiang B, Li X, Li G, and Xiong W. Trend analysis of cancer incidence and mortality in China. (2017) *Science China Life Sciences*. 60,1271-5.
3. Lian, Y.U., Xiong, F., Yang, L., Bo, H., Gong, Z., Wang, Y., Wei, F., Tang, Y., Li, X., Liao, Q. and Wang, H., (2018). Long noncoding RNA AFAP1-AS1 acts as a competing endogenous RNA of miR-423-5p to facilitate nasopharyngeal carcinoma metastasis through regulating the Rho/Rac pathway. *Journal of Experimental & Clinical Cancer Research*. 37, 1-17.
4. Wei, F., Wu, Y., Tang, L., He, Y., Shi, L., Xiong, F., Gong, Z., Guo, C., Li, X., Liao, Q. and Zhang, W., (2018) BPIFB1 (LPLUNC1) inhibits migration and invasion of nasopharyngeal carcinoma by interacting with VTN and VIM. *British journal of cancer*. 118, 233-247.
5. Deng, X., Xiong, F., Li, X., Xiang, B., Li, Z., Wu, X., Guo, C., Li, X., Li, Y., Li, G. and Xiong, W., (2018) Application of atomic force microscopy in cancer research. *Journal of nanobiotechnology*. 16, 1-15.
6. Najera, J., Rosenberger, M.R. and Datta, M., (2023) Atomic Force Microscopy Methods to Measure Tumor Mechanical Properties. *Cancers*, 15, 3285.
7. Magazzù, A. and Marcuello, C., (2023) Investigation of soft matter nanomechanics by atomic force microscopy and optical tweezers: A comprehensive review. *Nanomaterials*, 13, 963.
8. Laurent, V.M., Hénon, S., Planus, E., Fodil, R., Balland, M., Isabey, D. and Gallet, F.O., (2002) Assessment of mechanical properties of adherent living cells by bead micromanipulation: comparison of magnetic twisting cytometry vs optical tweezers. *J. Biomech. Eng.*, 124, 408-421.
9. Guck, J., Ananthakrishnan, R., Mahmood, H., Moon, T.J., Cunningham, C.C. and Käs, J., (2001) The optical stretcher: a novel laser tool to micromanipulate cells. *Biophysical journal*, 81, 767-784.
10. Weber, A., Benitez, R. and Toca-Herrera, J.L., (2022) Measuring biological materials mechanics with atomic force microscopy-Determination of viscoelastic cell properties from stress relaxation experiments. *Microscopy Research and Technique*, 85, 3284-3295.
- 11 Lal, R., Ramachandran, S. and Arnsdorf, M.F., (2010) Multidimensional atomic force microscopy: a versatile novel technology for nanopharmacology research. *The AAPS journal*, 12, 716-728.
12. Yang, F., Riedel, R., Del Pino, P., Pelaz, B., Said, A.H., Soliman, M., Pinnapireddy, S.R., Feliu, N., Parak, W.J., Bakowsky, U. and Hampp, N., (2017) Real-time, label-free monitoring of cell viability based on cell adhesion measurements with an atomic force microscope. *Journal of nanobiotechnology*, 15, 1-10.
13. Krieg, M., Fläschner, G., Alsteens, D., Gaub, B.M., Roos, W.H., Wuite, G.J., Gaub, H.E., Gerber, C., Dufrêne, Y.F. and Müller, D.J., (2019) Atomic force microscopy-based mechanobiology. *Nature Reviews Physics*, 1, 41-57.
14. Lekka, M., (2016) Discrimination between normal and cancerous cells using

AFM. *Bionanoscience*, 6, 65-80.

15. Prasad, S., Rankine, A., Prasad, T., Song, P., Dokukin, M.E., Makarova, N., Backman, V. and Sokolov, I., (2021) Atomic force microscopy detects the difference in cancer cells of different neoplastic aggressiveness via machine learning. *Advanced NanoBiomed Research*, 1, p.2000116.
16. Van der Meeren, L., Verduijn, J., Krysko, D.V. and Skirtach, A.G., (2020) AFM analysis enables differentiation between apoptosis, necroptosis, and ferroptosis in murine cancer cells. *Iscience*, 23.
17. Plodinec, M., Loparic, M., Monnier, C.A., Obermann, E.C., Zanetti-Dallenbach, R., Oertle, P., Hyotyla, J.T., Aebi, U., Bentires-Alj, M., Lim, R.Y. and Schoenenberger, C.A., (2012) The nanomechanical signature of breast cancer. *Nature nanotechnology*, 7, 757-765.
18. Lekka, M., (2012) A tip for diagnosing cancer. *Nature nanotechnology*, 7, 691-692.
19. Nia, H.T., Munn, L.L. and Jain, R.K., (2020) Physical traits of cancer. *Science*, 370, p.eaaz0868.
20. Northcott, J.M., Dean, I.S., Mouw, J.K. and Weaver, V.M., (2018) Feeling stress: the mechanics of cancer progression and aggression. *Frontiers in cell and developmental biology*, 6, 17.
21. Stylianou, A., Mpekris, F., Voutouri, C., Papoui, A., Constantinidou, A., Kitiris, E., Kailides, M. and Stylianopoulos, T., (2022) Nanomechanical properties of solid tumors as treatment monitoring biomarkers. *Acta Biomaterialia*, 154, 324-334.
22. Zhao, X., Zhong, Y., Ye, T., Wang, D. and Mao, B., (2015) Discrimination between cervical cancer cells and normal cervical cells based on longitudinal elasticity using atomic force microscopy. *Nanoscale research letters*, 10, 1-8.
23. He, Y.I., Jing, Y., Wei, F., Tang, Y., Yang, L., Luo, J., Yang, P., Ni, Q., Pang, J., Liao, Q. and Xiong, F., (2018). Long non-coding RNA PVT1 predicts poor prognosis and induces radioresistance by regulating DNA repair and cell apoptosis in nasopharyngeal carcinoma. *Cell death & disease*, 9, 235.
24. Tang, L., Wei, F., Wu, Y., He, Y., Shi, L., Xiong, F., Gong, Z., Guo, C., Li, X., Deng, H. and Cao, K., (2018) Role of metabolism in cancer cell radioresistance and radiosensitization methods. *Journal of Experimental & Clinical Cancer Research*, 37, 1-15.
25. Tang, Y., He, Y., Zhang, P., Wang, J., Fan, C., Yang, L., Xiong, F., Zhang, S., Gong, Z., Nie, S. and Liao, Q., (2018). LncRNAs regulate the cytoskeleton and related Rho/ROCK signaling in cancer metastasis. *Molecular cancer*, 17, 1-10.
26. Wei, F., Tang, L., He, Y., Wu, Y., Shi, L., Xiong, F., Gong, Z., Guo, C., Li, X., Liao, Q. and Zhang, W., (2018) BPIFB1 (LPLUNC1) inhibits radioresistance in nasopharyngeal carcinoma by inhibiting VTN expression. *Cell Death & Disease*, 9, 432.
27. Zhang, Y., Xia, M., Jin, K., Wang, S., Wei, H., Fan, C., Wu, Y., Li, X., Li, X., Li, G. and Zeng, Z., (2018) Function of the c-Met receptor tyrosine kinase in carcinogenesis and associated therapeutic opportunities. *Molecular cancer*, 17, 1-14.
28. Wang, Y.A., Li, X.L., Mo, Y.Z., Fan, C.M., Tang, L., Xiong, F., Guo, C., Xiang, B., Zhou, M., Ma, J. and Huang, X., (2018) Effects of tumor metabolic microenvironment on regulatory T cells. *Molecular cancer*, 17, 1-15.
29. Minelli, E., Ciasca, G., Sassun, T.E., Antonelli, M., Palmieri, V., Papi, M., Maulucci, G., Santoro,

- A., Giangaspero, F., Delfini, R. and Campi, G., (2017) A fully-automated neural network analysis of AFM force-distance curves for cancer tissue diagnosis. *Applied Physics Letters*, 111.
30. Fan, C., Tang, Y., Wang, J., Xiong, F., Guo, C., Wang, Y., Zhang, S., Gong, Z., Wei, F., Yang, L. and He, Y., (2017) Role of long non-coding RNAs in glucose metabolism in cancer. *Molecular cancer*, 16, 1-11.
31. Tu, C., Zeng, Z., Qi, P., Li, X., Yu, Z., Guo, C., Xiong, F., Xiang, B., Zhou, M., Gong, Z. and Liao, Q., (2017) Genome-wide analysis of 18 Epstein-Barr viruses isolated from primary nasopharyngeal carcinoma biopsy specimens. *Journal of virology*, 91, 10-1128.
32. Wang, J.P., Tang, Y.Y., Fan, C.M., Guo, C., Zhou, Y.H., Li, Z., Li, X.L., Li, Y., Li, G.Y., Xiong, W. and Zeng, Z.Y., (2018) The role of exosomal non-coding RNAs in cancer metastasis. *Oncotarget*, 9, 12487.
33. Yang, L., Tang, Y., Xiong, F., He, Y., Wei, F., Zhang, S., Guo, C., Xiang, B., Zhou, M., Xie, N. and Li, X., (2018) LncRNAs regulate cancer metastasis via binding to functional proteins. *Oncotarget*, 9, 1426.
34. Iwashita, M., Kataoka, N., Toida, K. and Kosodo, Y., (2014) Systematic profiling of spatiotemporal tissue and cellular stiffness in the developing brain. *Development*, 141, 3793-3798.
35. Sicard, D., Fredenburgh, L.E. and Tschumperlin, D.J., (2017). Measured pulmonary arterial tissue stiffness is highly sensitive to AFM indenter dimensions. *Journal of the mechanical behavior of biomedical materials*, 74, 118-127.
36. Sicard, D., Haak, A.J., Choi, K.M., Craig, A.R., Fredenburgh, L.E. and Tschumperlin, D.J., (2018) Aging and anatomical variations in lung tissue stiffness. *American Journal of Physiology-Lung Cellular and Molecular Physiology*, 314, L946-L955.
37. Zhu, Y., Dong, Z., Wejinya, U.C., Jin, S. and Ye, K., (2011) Determination of mechanical properties of soft tissue scaffolds by atomic force microscopy nanoindentation. *Journal of biomechanics*, 44, 2356-2361.
38. Mao, Y., Sun, Q., Wang, X., Ouyang, Q., Han, L., Jiang, L. and Han, D., (2009) In vivo nanomechanical imaging of blood-vessel tissues directly in living mammals using atomic force microscopy. *Applied Physics Letters*, 95.
39. Kontomaris, S.V., Malamou, A. and Stylianou, A., (2020) A new approach for the AFM-based mechanical characterization of biological samples. *Scanning*, 2020.
40. Qian, L. and Zhao, H., (2018) Nanoindentation of soft biological materials. *Micromachines*, 9, 654.
41. Kontomaris, S.V., Malamou, A. and Stylianou, A., (2022) The Hertzian theory in AFM nanoindentation experiments regarding biological samples: Overcoming limitations in data processing. *Micron*, 155, p.103228.
42. Pogoda, K., Jaczewska, J., Wiltowska-Zuber, J., Klymenko, O., Zuber, K., Fornal, M. and Lekka, M., (2012) Depth-sensing analysis of cytoskeleton organization based on AFM data. *European Biophysics Journal*, 41, 79-87.
43. Pogoda, K., Jaczewska, J., Wiltowska-Zuber, J., Klymenko, O., Zuber, K., Fornal, M. and Lekka,

- M., (2012). Depth-sensing analysis of cytoskeleton organization based on AFM data. *European Biophysics Journal*, 41, 79-87.
44. Ding, Y., Wang, J., Xu, G.K. and Wang, G.F., (2018) Are elastic moduli of biological cells depth dependent or not? Another explanation using a contact mechanics model with surface tension. *Soft Matter*, 14, 7534-7541.
45. Xia, F. and Youcef-Toumi, K. (2022) Advanced Atomic Force Microscopy Modes for Biomedical Research. *Biosensors*. 12,1116-1140.
46. Sifat, A.A., Jahng, J. and Potma, E.O. (2022) Photo-induced force microscopy (PiFM)—principles and implementations. *Chemical Society Reviews*. 51, 4208-4222.
47. Dazzi, A., Prazeres, R., Glotin, F. and Ortega, J.M. (2005) Local infrared microspectroscopy with subwavelength spatial resolution with an atomic force microscope tip used as a photothermal sensor. *Optics letters*. 30,2388-2390.
48. Lu, F., Jin, M. and Belkin, M.A. (2014) Tip-enhanced infrared nanospectroscopy via molecular expansion force detection. *Nature photonics*. 8, 307-312.
49. Nowak, D., Morrison, W., Wickramasinghe, H.K., Jahng, J., Potma, E., Wan, L., Ruiz, R., Albrecht, T.R., Schmidt, K., Frommer, J. and Sanders, D.P. (2016) Nanoscale chemical imaging by photoinduced force microscopy. *Science advances*. 2, 1501571.
50. Pürckhauer, K., Weymouth, A.J., Pfeiffer, K., Kullmann, L., Mulvihill, E., Krahn, M.P., Müller, D.J. and Giessibl, F.J. (2018) Imaging in biologically-relevant environments with AFM using stiff qPlus sensors. *Scientific Reports*. 8, 9330.
51. Xia, F., Yang, C., Wang, Y., Youcef-Toumi, K., Reuter, C., Ivanov, T., Holz, M. and Rangelow, I.W. (2019) Lights out! nano-scale topography imaging of sample surface in opaque liquid environments with coated active cantilever probes. *Nanomaterials*. 9, 1013.
52. Viji Babu, P.K. and Radmacher, M. (2019) Mechanics of brain tissues studied by atomic force microscopy: A perspective. *Frontiers in Neuroscience*.13, 600.
53. Stolz, M., Raiteri, R., Daniels, A.U., VanLandingham, M.R., Baschong, W. and Aebi, U. (2004) Dynamic elastic modulus of porcine articular cartilage determined at two different levels of tissue organization by indentation-type atomic force microscopy. *Biophysical journal*. 86, 3269-3283.
54. Thavarajah, R., Mudimbaimannar, V.K., Elizabeth, J., Rao, U.K. and Ranganathan, K. (2012) Chemical and physical basics of routine formaldehyde fixation. *Journal of oral and maxillofacial pathology*. 16, 400-405.
55. Troiano, N.W., Ciovacco, W.A. and Kacena, M.A. (2009) The effects of fixation and dehydration on the histological quality of undecalcified murine bone specimens embedded in methylmethacrylate. *Journal of histotechnology*. 32, 27.
56. Fischer, A.H., Jacobson, K.A., Rose, J. and Zeller, R. (2008) Cryosectioning tissues. *CSH Protoc* 2008: prot4991.
57. Navindaran, K., Kang, J.S. and Moon, K. (2023) Techniques for characterizing mechanical properties of soft tissues. *Journal of the Mechanical Behavior of Biomedical Materials*. 138, 105575.

58. Farniev, V.M., Shmelev, M.E., Shved, N.A., Gulaia, V.S., Biktimirov, A.R., Zhizhchenko, A.Y., Kuchmizhak, A.A. and Kumeiko, V.V. (2022) Nanomechanical and morphological afm mapping of normal tissues and tumors on live brain slices using specially designed embedding matrix and laser-shaped cantilevers. *Biomedicines*. 10,1742.
59. Stolz, M., Raiteri, R., Daniels, A.U., VanLandingham, M.R., Baschong, W. and Aebi, U. (2004) Dynamic elastic modulus of porcine articular cartilage determined at two different levels of tissue organization by indentation-type atomic force microscopy. *Biophysical journal*. 86, 3269-3283.
60. Mao, Y., Sun, Q., Wang, X., Ouyang, Q., Han, L., Jiang, L. and Han, D. (2009) In vivo nanomechanical imaging of blood-vessel tissues directly in living mammals using atomic force microscopy. *Applied Physics Letters*, 95.
61. Plodinec, M., Loparic, M., Monnier, C.A., Obermann, E.C., Zanetti-Dallenbach, R., Oertle, P., Hyotyla, J.T., Aebi, U., Bentires-Alj, M., Lim, R.Y. and Schoenenberger, C.A. (2012) The nanomechanical signature of breast cancer. *Nature nanotechnology*. 7, 757-765.
62. Tian, M., Li, Y., Liu, W., Jin, L., Jiang, X., Wang, X., Ding, Z., Peng, Y., Zhou, J., Fan, J. and Cao, Y. (2015) The nanomechanical signature of liver cancer tissues and its molecular origin. *Nanoscale*. 7, 12998-13010.
63. Meister, A., Gabi, M., Behr, P., Studer, P., Vörös, J., Niedermann, P., Bitterli, J., Polesel-Maris, J., Liley, M., Heinzemann, H. and Zambelli, T. (2009) FluidFM: combining atomic force microscopy and nanofluidics in a universal liquid delivery system for single cell applications and beyond. *Nano letters*. 9, 2501-2507.
64. Li, W., Sancho, A., Chung, W.L., Vinik, Y., Groll, J., Zick, Y., Medalia, O., Bershadsky, A.D. and Geiger, B. (2021) Differential cellular responses to adhesive interactions with galectin-8-and fibronectin-coated substrates. *Journal of Cell Science*, 134, jcs252221.
65. Sztilkovics, M., Gerecsei, T., Peter, B., Saftics, A., Kurunczi, S., Szekacs, I., Szabo, B. and Horvath, R. (2020) Single-cell adhesion force kinetics of cell populations from combined label-free optical biosensor and robotic fluidic force microscopy. *Scientific reports*. 10, 61.
66. Mathelié-Guinlet, M., Viela, F., Dehullu, J., Filimonava, S., Rauceo, J.M., Lipke, P.N. and Dufrêne, Y.F. (2021) Single-cell fluidic force microscopy reveals stress-dependent molecular interactions in yeast mating. *Communications Biology*. 4, 33.
67. Li, M., Liu, L. and Zambelli, T. (2022) FluidFM for single-cell biophysics. *Nano Research*. 15, 773-786.
68. Guillaume-Gentil, O., Potthoff, E., Ossola, D., Dörig, P., Zambelli, T. and Vorholt, J.A. (2013) Force-controlled fluidic injection into single cell nuclei. *Small*. 9, 1904-1907.
69. Higgins, S.G. and Stevens, M.M. (2017) Extracting the contents of living cells. *Science*, 356, 379-380.
70. Guillaume-Gentil, O., Grindberg, R.V., Kooger, R., Dorwling-Carter, L., Martinez, V., Ossola, D., Pilhofer, M., Zambelli, T. and Vorholt, J.A. (2016) Tunable single-cell extraction for molecular analyses. *Cell*. 166, 506-516.

71. Guillaume-Gentil, O., Rey, T., Kiefer, P., Ibáñez, A.J., Steinhoff, R., Brönnimann, R., Dorwling-Carter, L., Zambelli, T., Zenobi, R. and Vorholt, J.A. (2017) Single-cell mass spectrometry of metabolites extracted from live cells by fluidic force microscopy. *Analytical Chemistry*, 89, 5017-5023.
72. Verkman, A.S., (2012) Aquaporins in clinical medicine. *Annual review of medicine*, 63, 303-316.
73. Kruse, E., Uehlein, N. and Kaldenhoff, R., (2006) The aquaporins. *Genome biology*, 7, 1-6.
74. Prata, C., Hrelia, S. and Fiorentini, D., (2019) Peroxiporins in cancer. *International Journal of Molecular Sciences*, 20, 1371.
75. Kuroczycki-Saniutycz S, Grzeszczuk A, Zwierz ZW, Kołodziejczyk P, Szczesiul J, Zalewska-Szajda B, Ościłowicz K, Waszkiewicz N, Zwierz K, Szajda SD. Prevention of pancreatic cancer. *Contemporary Oncology/Współczesna Onkologia*. 2017 Feb;21(1):30-4.
76. Silva, P.M., da Silva, I.V., Sarmiento, M.J., Silva, Í.C., Carvalho, F.A., Soveral, G. and Santos, N.C., (2022) Aquaporin-3 and Aquaporin-5 Facilitate Migration and Cell–Cell Adhesion in Pancreatic Cancer by Modulating Cell Biomechanical Properties. *Cells*, 11, 1308.
77. Prat, J., (2012) Ovarian carcinomas: five distinct diseases with different origins, genetic alterations, and clinicopathological features. *Virchows Archiv*, 460, 237-249.
78. Macintyre, G., Goranova, T.E., De Silva, D., Ennis, D., Piskorz, A.M., Eldridge, M., Sie, D., Lewsley, L.A., Hanif, A., Wilson, C. and Dowson, S., (2018) Copy number signatures and mutational processes in ovarian carcinoma. *Nature genetics*, 50, 1262-1270.
79. Tothill, R.W., Tinker, A.V., George, J., Brown, R., Fox, S.B., Lade, S., Johnson, D.S., Trivett, M.K., Etemadmoghadam, D., Locandro, B. and Traficante, N., 2008. Novel molecular subtypes of serous and endometrioid ovarian cancer linked to clinical outcome. *Clinical cancer research*, 14, 5198-5208.
80. Köbel, M., Bak, J., Bertelsen, B.I., Carpen, O., Grove, A., Hansen, E.S., Levin Jakobsen, A.M., Lidang, M., Måsbäck, A., Tolf, A. and Gilks, C.B., (2014) Ovarian carcinoma histotype determination is highly reproducible, and is improved through the use of immunohistochemistry. *Histopathology*, 64, 1004-1013.
81. Murakami, R., Matsumura, N., Mandai, M., Yoshihara, K., Tanabe, H., Nakai, H., Yamanoi, K., Abiko, K., Yoshioka, Y., Hamanishi, J. and Yamaguchi, K., (2016) Establishment of a novel histopathological classification of high-grade serous ovarian carcinoma correlated with prognostically distinct gene expression subtypes. *The American journal of pathology*, 186, 1103-1113.
82. Kalimuthu, S.N., Wilson, G.W., Grant, R.C., Seto, M., O’Kane, G., Vajpeyi, R., Notta, F., Gallinger, S. and Chetty, R., (2019) Morphological classification of pancreatic ductal adenocarcinoma that predicts molecular subtypes and correlates with clinical outcome. *Gut*, pp.gutjnl-2019.
83. Shia, J., Schultz, N., Kuk, D., Vakiani, E., Middha, S., Segal, N.H., Hechtman, J.F., Berger, M.F., Stadler, Z.K., Weiser, M.R. and Wolchok, J.D., (2017). Morphological characterization of colorectal cancers in The Cancer Genome Atlas reveals distinct morphology–molecular associations: clinical and biological implications. *Modern pathology*, 30, 599-609.
84. Azzalini, E., Abdurakhmanova, N., Parris, P., Bartoletti, M., Canzonieri, V., Stanta, G., Casalis, L. and Bonin, S., (2021) Cell-stiffness and morphological architectural patterns in clinical samples of high

- grade serous ovarian cancers. *Nanomedicine: Nanotechnology, Biology and Medicine*, 37, 102452.
85. Cross SE, Jin YS, Rao J, Gimzewski JK. Nanomechanical analysis of cells from cancer patients. *In Nano-enabled medical applications 2020 Nov 23* (pp. 547-566). Jenny Stanford Publishing.
86. Lekka, M., Laidler, P., Gil, D., Lekki, J., Stachura, Z. and Hryniewicz, A.Z., (1999) Elasticity of normal and cancerous human bladder cells studied by scanning force microscopy. *European Biophysics Journal*, 28, 312-316.
87. Lekka, M., Pogoda, K., Gostek, J., Klymenko, O., Prauzner-Bechcicki, S., Wiltowska-Zuber, J., Jaczewska, J., Lekki, J. and Stachura, Z., (2012). Cancer cell recognition–mechanical phenotype. *Micron*, 43, 1259-1266.
88. Culp, M.B., Soerjomataram, I., Efstathiou, J.A., Bray, F. and Jemal, A., (2020) Recent global patterns in prostate cancer incidence and mortality rates. *European urology*, 77, 38-52.
89. Swami, U., McFarland, T.R., Nussenzeig, R. and Agarwal, N., (2020) Advanced prostate cancer: treatment advances and future directions. *Trends in cancer*, 6, 702-715.
90. Teo, M.Y., Rathkopf, D.E. and Kantoff, P., (2019). Treatment of advanced prostate cancer. *Annual review of medicine*, 70, 479-499.
91. Jin J. Screening for prostate cancer. *Jama*. 2018 May 8;319(18):1946-.
92. Ghosh, D. and Dawson, M.R., (2018). Microenvironment influences cancer cell mechanics from tumor growth to metastasis. *Biomechanics in oncology*, 69-90.
93. Kalli, M. and Stylianopoulos, T., (2018) Defining the role of solid stress and matrix stiffness in cancer cell proliferation and metastasis. *Frontiers in oncology*, 8, 55.
94. Gil-Redondo, J.C., Weber, A., Zbiral, B. and Toca-Herrera, J.L., (2022). Substrate stiffness modulates the viscoelastic properties of MCF-7 cells. *Journal of the Mechanical Behavior of Biomedical Materials*, 125, 104979.
95. Rouvière, O., Melodelima, C., Hoang Dinh, A., Bratan, F., Pagnoux, G., Sanzalone, T., Crouzet, S., Colombel, M., Mège-Lechevallier, F. and Souchon, R., (2017) Stiffness of benign and malignant prostate tissue measured by shear-wave elastography: a preliminary study. *European radiology*, 27, 1858-1866.
96. Zhai, L., Madden, J., Foo, W.C., Mouraviev, V., Polascik, T.J., Palmeri, M.L. and Nightingale, K.R., (2010) Characterizing stiffness of human prostates using acoustic radiation force. *Ultrasonic imaging*, 32, 201-213.
97. Junker, D., De Zordo, T., Quentin, M., Ladurner, M., Bektic, J., Horniger, W., Jaschke, W. and Aigner, F., (2014) Real-time elastography of the prostate. *BioMed research international*, 2014.
98. Tang, X., Zhang, Y., Mao, J., Wang, Y., Zhang, Z., Wang, Z. and Yang, H., (2022) Effects of substrate stiffness on the viscoelasticity and migration of prostate cancer cells examined by atomic force microscopy. *Beilstein Journal of Nanotechnology*, 13, 560-569.
99. Sung, H., Ferlay, J., Siegel, R.L., Laversanne, M., Soerjomataram, I., Jemal, A. and Bray, F., 2021. Global cancer statistics (2020): GLOBOCAN estimates of incidence and mortality worldwide for 36 cancers in 185 countries. *CA: a cancer journal for clinicians*, 71, 209-249.

100. Singh, J., Hussain, Y., Luqman, S. and Meena, A., (2019) Targeting Ca²⁺ signalling through phytochemicals to combat cancer. *Pharmacological Research*, 146, 104282.
101. Shussman, N. and Wexner, S.D., (2014). Colorectal polyps and polyposis syndromes. *Gastroenterology report*, 2, 1-15.
102. Thiery, J.P., Acloque, H., Huang, R.Y. and Nieto, M.A., (2009) Epithelial-mesenchymal transitions in development and disease. *cell*, 139, 871-890.
103. Stuelten, C.H., Parent, C.A. and Montell, D.J., (2018). Cell motility in cancer invasion and metastasis: insights from simple model organisms. *Nature Reviews Cancer*, 18, 296-312.
104. Brás, M.M., Cruz, T.B., Maia, A.F., Oliveira, M.J., Sousa, S.R., Granja, P.L. and Radmacher, M., (2022) Mechanical properties of colorectal cancer cells determined by dynamic atomic force microscopy: a novel biomarker. *Cancers*, 14, 5053.
105. Stylianou, A., Voutouri, C., Mpekris, F. and Stylianopoulos, T., (2023) Pancreatic Cancer Presents Distinct Nanomechanical Properties During Progression. *Annals of Biomedical Engineering*, 1-14.
106. Luo, Q., Kuang, D., Zhang, B. and Song, G., (2016) Cell stiffness determined by atomic force microscopy and its correlation with cell motility. *Biochimica et Biophysica Acta (BBA)-General Subjects*, 1860, 1953-1960.
107. Jaumouillé, V. and Waterman, C.M., (2020). Physical constraints and forces involved in phagocytosis. *Frontiers in immunology*, 11, 1097.
108. Raudenska M, Kratochvilova M, Vicar T, Gumulec J, Balvan J, Polanska H, Pribyl J, Masarik M. Cisplatin enhances cell stiffness and decreases invasiveness rate in prostate cancer cells by actin accumulation. *Scientific reports*. 2019 Feb 7;9(1):1660.
110. Herbst, R.S. and Khuri, F.R., (2003) Mode of action of docetaxel—a basis for combination with novel anticancer agents. *Cancer treatment reviews*, 29, 407-415.
111. Köpf-Maier, P. and Mühlhausen, S.K., (1992) Changes in the cytoskeleton pattern of tumor cells by cisplatin in vitro. *Chemico-biological interactions*, 82, 295-316.
112. Boekelheide, K., Arcila, M.E. and Eveleth, J., (1992) cis-diamminedichloroplatinum (II)(cisplatin) alters microtubule assembly dynamics. *Toxicology and applied pharmacology*, 116, 146-151.
113. Gumulec, J., Masarik, M., Krizkova, S., Adam, V., Hubalek, J., Hrabeta, J., Eckschlager, T., Stiborova, M. and Kizek, R., 2011. Insight to physiology and pathology of zinc (II) ions and their actions in breast and prostate carcinoma. *Current medicinal chemistry*, 18, 5041-5051.
114. Franklin, R.B. and Costello, L.C., (2009). The important role of the apoptotic effects of zinc in the development of cancers. *Journal of cellular biochemistry*, 106, 750-757.
115. Kratochvilova, M., Raudenska, M., Heger, Z., Richtera, L., Cernei, N., Adam, V., Babula, P., Novakova, M., Masarik, M. and Gumulec, J., (2017). Amino acid profiling of zinc resistant prostate cancer cell lines: associations with cancer progression. *The Prostate*, 77, 604-616..
116. Lin, H.H., Lin, H.K., Lin, I.H., Chiou, Y.W., Chen, H.W., Liu, C.Y., Hans, I., Harn, C., Chiu, W.T., Wang, Y.K. and Shen, M.R., (2015). Mechanical phenotype of cancer cells: cell softening and loss of

stiffness sensing. *Oncotarget*, 6, 20946.

117. Yang, B., Radel, C., Hughes, D., Kelemen, S. and Rizzo, V., (2011). p190 RhoGTPase-activating protein links the β 1 integrin/caveolin-1 mechanosignaling complex to RhoA and actin remodeling. *Arteriosclerosis, thrombosis, and vascular biology*, 31, 376-383.

118. Rotsch, C. and Radmacher, M., (2000) Drug-induced changes of cytoskeletal structure and mechanics in fibroblasts: an atomic force microscopy study. *Biophysical journal*, 78, 520-535.

119. Bastatas, L., Martinez-Marin, D., Matthews, J., Hashem, J., Lee, Y.J., Sennoune, S., Filleur, S., Martinez-Zaguilan, R. and Park, S., (2012). AFM nano-mechanics and calcium dynamics of prostate cancer cells with distinct metastatic potential. *Biochimica et Biophysica Acta (BBA)-General Subjects*, 1820, 1111-1120.

120. Denais, C. and Lammerding, J., (2014). Nuclear mechanics in cancer. *Cancer biology and the nuclear envelope: Recent advances may elucidate past paradoxes*, 435-470.

121. Rao, K.M.K. and Cohen, H.J., (1991) Actin cytoskeletal network in aging and cancer. *Mutation Research/DNAging*, 256, 139-148.

122. Thoumine, O. and Ott, A., (1997). Comparison of the mechanical properties of normal and transformed fibroblasts. *Biorheology*, 34, 309-326.

123. Lekka, M., Laidler, P., Gil, D., Lekki, J., Stachura, Z. and Hryniewicz, A.Z., (1999). Elasticity of normal and cancerous human bladder cells studied by scanning force microscopy. *European Biophysics Journal*, 28, 312-316.

124. Alibert, C., Goud, B. and Manneville, J.B., (2017) Are cancer cells really softer than normal cells?. *Biology of the Cell*, 109, 167-189.

125. Sharma, S., Santiskulvong, C., Bentolila, L.A., Rao, J., Dorigo, O. and Gimzewski, J.K., (2012) Correlative nanomechanical profiling with super-resolution F-actin imaging reveals novel insights into mechanisms of cisplatin resistance in ovarian cancer cells. *Nanomedicine: Nanotechnology, Biology and Medicine*, 8, 757-766.

126. Lam, W.A., Rosenbluth, M.J. and Fletcher, D.A., (2007) Chemotherapy exposure increases leukemia cell stiffness. *Blood*, 109, 3505-3508.

127. Chaudhuri, O., Parekh, S.H., Lam, W.A. and Fletcher, D.A., (2009) Combined atomic force microscopy and side-view optical imaging for mechanical studies of cells. *Nature methods*, 6, 383-387.

128. Fletcher, D.A. and Mullins, R.D., (2010). Cell mechanics and the cytoskeleton. *Nature*, 463, 485-492.

129. Sun, M., Graham, J.S., Hegedüs, B., Marga, F., Zhang, Y., Forgacs, G. and Grandbois, M., (2005) Multiple membrane tethers probed by atomic force microscopy. *Biophysical journal*, 89, 4320-4329.

130. Rieder, C.L. and Maiato, H., (2004). Stuck in division or passing through: what happens when cells cannot satisfy the spindle assembly checkpoint. *Developmental cell*, 7, 637-651.

131. Yun, X., Tang, M., Yang, Z., Wilksch, J.J., Xiu, P., Gao, H., Zhang, F. and Wang, H., (2017) Interrogation of drug effects on HeLa cells by exploiting new AFM mechanical biomarkers. *RSC advances*, 7, 43764-43771.

132. Li, J., Wijeratne, S.S., Nelson, T.E., Lin, T.C., He, X., Feng, X., Nikoloutsos, N., Fang, R., Jiang, K., Lian, I. and Kiang, C.H., (2020) Dependence of membrane tether strength on substrate rigidity probed by single-cell force spectroscopy. *The Journal of Physical Chemistry Letters*, 11, 4173-4178.
133. de Alcântara-Contessoto NS, Cornélio ML, Kiang CH. Quantifying the effect of anti-cancer compound (piperlongumine) on cancer cells using single-cell force spectroscopy. *bioRxiv*. 2021 Sep 6:2021-09.
134. Berg, D.R., Colombel, J.F. and Ungaro, R., (2019). The role of early biologic therapy in inflammatory bowel disease. *Inflammatory bowel diseases*, 25, 1896-1905.
135. Papamichael, K., Lin, S., Moore, M., Papaioannou, G., Sattler, L. and Cheifetz, A.S., (2019) Infliximab in inflammatory bowel disease. *Therapeutic advances in chronic disease*, 10, 2040622319838443.
136. Franca, R., Curci, D., Lucafo, M., Decorti, G. and Stocco, G., (2019) Therapeutic drug monitoring to improve outcome of anti-TNF drugs in pediatric inflammatory bowel disease. *Expert Opinion on Drug Metabolism & Toxicology*, 15, 527-539.
137. Nasser, Y., Labetoulle, R., Harzallah, I., Berger, A.E., Roblin, X. and Paul, S., (2018) Comparison of point-of-care and classical immunoassays for the monitoring infliximab and antibodies against infliximab in IBD. *Digestive Diseases and Sciences*, 63, 2714-2721.
138. Castele, N.V., (2016). Assays for measurement of TNF antagonists in practice. *Frontline Gastroenterology*, pp.flgastro-2016.
139. Curci, D., Lucafo, M., Parisse, P., Decorti, G., Bramuzzo, M., Casalis, L. and Stocco, G., (2022). Atomic force microscopy application for the measurement of infliximab concentration in healthy donors and pediatric patients with inflammatory bowel disease. *Journal of Personalized Medicine*, 12, 948.
140. Stylianou, A., Mpekris, F., Voutouri, C., Papoui, A., Constantinidou, A., Kitiris, E., Kailides, M. and Stylianopoulos, T., (2022) Nanomechanical properties of solid tumors as treatment monitoring biomarkers. *Acta Biomaterialia*, 154, 324-334.
141. Matusovsky, O.S., Kodera, N., MacEachen, C., Ando, T., Cheng, Y.S. and Rassier, D.E. (2020) Millisecond conformational dynamics of skeletal myosin II power stroke studied by high-speed atomic force microscopy. *ACS nano*. 15, 2229-2239.
142. Adams, J.D., Nievergelt, A., Erickson, B.W., Yang, C., Dukic, M. and Fantner, G.E. (2014) High-speed imaging upgrade for a standard sample scanning atomic force microscope using small cantilevers. *Review of Scientific Instruments*. 85.
143. Braunsman, C., Seifert, J., Rheinlaender, J. and Schäffer, T.E. (2014.) High-speed force mapping on living cells with a small cantilever atomic force microscope. *Review of Scientific Instruments*. 85.
144. Pedrak, R., Ivanov, T., Ivanova, K., Gotszalk, T., Abedinov, N., Rangelow, I.W., Edinger, K., Tomerov, E., Schenkel, T. and Hudek, P. (2003) Micromachined atomic force microscopy sensor with integrated piezoresistive sensor and thermal bimorph actuator for high-speed tapping-mode atomic force microscopy phase-imaging in higher eigenmodes. *Journal of Vacuum Science & Technology B: Microelectronics and Nanometer Structures Processing, Measurement, and Phenomena*, 21, 3102-3107.

145. Mohamed, M.S., Hazawa, M., Kobayashi, A., Guillaud, L., Watanabe-Nakayama, T., Nakayama, M., Wang, H., Kodera, N., Oshima, M., Ando, T. and Wong, R.W. (2020) Spatiotemporally tracking of nano-biofilaments inside the nuclear pore complex core. *Biomaterials*. 256,120198.
146. Umakoshi, T., Fukuda, S., Iino, R., Uchihashi, T. and Ando, T. (2020) High-speed near-field fluorescence microscopy combined with high-speed atomic force microscopy for biological studies. *Biochimica et Biophysica Acta (BBA)-General Subjects*, 1864, 29325.
147. Walters, D.A., Cleveland, J.P., Thomson, N.H., Hansma, P.K., Wendman, M.A., Gurley, G. and Elings, V. (1996) Short cantilevers for atomic force microscopy. *Review of Scientific Instruments*, 67, 3583-3590.
148. Schäffer, T.E., Cleveland, J.P., Ohnesorge, F., Walters, D.A. and Hansma, P.K. (1996) Studies of vibrating atomic force microscope cantilevers in liquid. *Journal of applied physics*, 80, 3622-3627.
149. Viani, M.B., Schäffer, T.E., Palocz, G.T., Pietrasanta, L.I., Smith, B.L., Thompson, J.B., Richter, M., Rief, M., Gaub, H.E., Plaxco, K.W. and Cleland, A.N. (1999) Fast imaging and fast force spectroscopy of single biopolymers with a new atomic force microscope designed for small cantilevers. *Review of Scientific Instruments*. 70, 4300-4303.
150. Ando, T., Kodera, N., Takai, E., Maruyama, D., Saito, K. and Toda, A. (2001) A high-speed atomic force microscope for studying biological macromolecules. *Proceedings of the National Academy of Sciences*. 98, 12468-12472.
151. Humphris, A.D.L., Miles, M.J. and Hobbs, J.K. (2005) A mechanical microscope: High-speed atomic force microscopy. *Applied physics letters*. 86.
152. Leitner, M., Fantner, G.E., Fantner, E.J., Ivanova, K., Ivanov, T., Rangelow, I., Ebner, A., Rangl, M., Tang, J. and Hinterdorfer, P. (2012) Increased imaging speed and force sensitivity for bio-applications with small cantilevers using a conventional AFM setup. *Micron*. 43, 1399-1407.
153. Schitter, G., Astrom, K.J., DeMartini, B.E., Thurner, P.J., Turner, K.L. and Hansma, P.K. (2007) Design and modeling of a high-speed AFM-scanner. *IEEE Transactions on Control Systems Technology*. 15, 906-915.
154. Braunsman, C. and Schäffer, T.E. (2010) High-speed atomic force microscopy for large scan sizes using small cantilevers. *Nanotechnology*. 21, 225705.
155. Fischer-Friedrich, E., Toyoda, Y., Cattin, C.J., Müller, D.J., Hyman, A.A. and Jülicher, F. (2016) Rheology of the active cell cortex in mitosis. *Biophysical journal*. 111, 589-600.
156. Schächtele, M., Kemmler, J., Rheinlaender, J. and Schäffer, T.E. (2022) Combined High-Speed Atomic Force and Optical Microscopy Shows That Viscoelastic Properties of Melanoma Cancer Cells Change during the Cell Cycle. *Advanced Materials Technologies*. 7, 2101000.
157. Zhao, J., Zeng, H., Kalia, S. and Lui, H. (2017) Using Raman spectroscopy to detect and diagnose skin cancer in vivo. *Dermatologic Clinics*. 35, 495-504.
158. Tsikritsis, D., Richmond, S., Stewart, P., Elfick, A. and Downes, A. (2015) Label-free identification and characterization of living human primary and secondary tumour cells. *Analyst*, 140, 5162-5168.
159. Zhang, H., Xiao, L., Li, Q., Qi, X. and Zhou, A. (2018) Microfluidic chip for non-invasive analysis

of tumor cells interaction with anti-cancer drug doxorubicin by AFM and Raman spectroscopy. *Biomicrofluidics*, 12.

160. Kopeć, M. and Abramczyk, H. (2018) Angiogenesis-a crucial step in breast cancer growth, progression and dissemination by Raman imaging. *Spectrochimica Acta Part A: Molecular and Biomolecular Spectroscopy*, 198, 338-345.

161. Abramczyk, H., Imiela, A., Brozek-Pluska, B. and Kopeć, M. (2019) Advances in Raman imaging combined with AFM and fluorescence microscopy are beneficial for oncology and cancer research. *Nanomedicine*, 14, 1873-1888.

162. Beton, K., Wysocki, P. and Brozek-Pluska, B. (2022) Mevastatin in colon cancer by spectroscopic and microscopic methods—Raman imaging and AFM studies. *Spectrochimica Acta Part A: Molecular and Biomolecular Spectroscopy*, 270, 120726.

163. Staunton, J.R., Doss, B.L. and Ros, R. (2014) Combined Clsm and afm indentation reveals metastatic cancer cells stiffen during Rho/ROCK contractility-dependent invasion of collagen I matrices. *Biophysical Journal*, 106, 176a.

164. Fuhrmann, A., Staunton, J.R., Nandakumar, V., Banyai, N., Davies, P.C.W. and Ros, R. (2011) AFM stiffness nanotomography of normal, metaplastic and dysplastic human esophageal cells. *Physical biology*, 8, 015007.

165. Capello, M., Ferri-Borgogno, S., Cappello, P. and Novelli, F. (2011) α -enolase: a promising therapeutic and diagnostic tumor target. *The FEBS journal*, 278, 1064-1074.

166. Díaz-Ramos, À., Roig-Borrellas, A., García-Melero, A. and López-Aleman, R. (2012) α -Enolase, a multifunctional protein: its role on pathophysiological situations. *BioMed Research International*.

167. Principe, M., Borgoni, S., Cascione, M., Chattaragada, M.S., Ferri-Borgogno, S., Capello, M., Bulfamante, S., Chapelle, J., Di Modugno, F., Defilippi, P. and Nisticò, P. (2017) Alpha-enolase (ENO1) controls α v/ β 3 integrin expression and regulates pancreatic cancer adhesion, invasion, and metastasis. *Journal of hematology & oncology*, 10, 1-13.

168. Vahabi, S., Salman, B.N. and Javanmard, A. (2013) Atomic force microscopy application in biological research: a review study. *Iranian journal of medical sciences*, 38, 76.

169. Krieg, M., Fläschner, G., Alsteens, D., Gaub, B.M., Roos, W.H., Wuite, G.J., Gaub, H.E., Gerber, C., Dufrêne, Y.F. and Müller, D.J. (2019) Atomic force microscopy-based mechanobiology. *Nature Reviews Physics*, 1, 41-57.

170. Vahabi, S., Salman, B.N. and Javanmard, A., (2013). Atomic force microscopy application in biological research: a review study. *Iranian journal of medical sciences*, 38, 76.

171. Uchihashi, T., Iino, R., Ando, T. and Noji, H., (2011). High-speed atomic force microscopy reveals rotary catalysis of rotorless F1-ATPase. *Science*, 333, 755-758.

172. Adamcik, J., Berquand, A. and Mezzenga, R., (2011). Single-step direct measurement of amyloid fibrils stiffness by peak force quantitative nanomechanical atomic force microscopy. *Applied Physics Letters*, 98.

173. Calzado-Martín, A., Encinar, M., Tamayo, J., Calleja, M. and San Paulo, A., (2016). Effect of actin

organization on the stiffness of living breast cancer cells revealed by peak-force modulation atomic force microscopy. *ACS nano*, 10, 3365-3374.

174. Vargas-Pinto, R., Gong, H., Vahabikashi, A. and Johnson, M., (2013). The effect of the endothelial cell cortex on atomic force microscopy measurements. *Biophysical journal*, 105, 00-309.

175. Abraham, A., Mihaliuk, E., Kumar, B., Legleiter, J. and Gullion, T. (2010) Solid-state NMR study of cysteine on gold nanoparticles. *The Journal of Physical Chemistry C*, 114, 18109-18114.

176. Kumar, B., Pifer, P.M., Giovengo, A. and Legleiter, J. (2010). The effect of set point ratio and surface Young's modulus on maximum tapping forces in fluid tapping mode atomic force microscopy. *Journal of Applied Physics*, 107.

177. Kumar, B., Miller, K., Charon, N.W. and Legleiter, J. (2017). Periplasmic flagella in *Borrelia burgdorferi* function to maintain cellular integrity upon external stress. *Plos one*, 12, e0184648.

178. Lekka, M., (2016). Discrimination between normal and cancerous cells using AFM. *Bionanoscience*, 6, 65-80.

179. Radmacher, M., 2007. Studying the mechanics of cellular processes by atomic force microscopy. *Methods in cell biology*, 83, 347-372.

180. Gavara, N., (2016). Combined strategies for optimal detection of the contact point in AFM force-indentation curves obtained on thin samples and adherent cells. *Scientific reports*, 6, 21267.

181. Churnside, A.B. and Perkins, T.T., (2014). Ultrastable atomic force microscopy: improved force and positional stability. *FEBS letters*, 588, 3621-3630.

182. King, G.M., Carter, A.R., Churnside, A.B., Eberle, L.S. and Perkins, T.T., (2009). Ultrastable atomic force microscopy: atomic-scale stability and registration in ambient conditions. *Nano letters*, 9, 1451-1456.

183. Quail, D.F. and Joyce, J.A., 2013. Microenvironmental regulation of tumor progression and metastasis. *Nature medicine*, 19, 1423-1437.

184. Di Carlo, D. (2012) A mechanical biomarker of cell state in medicine. *Journal of laboratory automation*, 17, 32-42.

185. Heu, C., Berquand, A., Elie-Caille, C. and Nicod, L. (2012) Glyphosate-induced stiffening of HaCaT keratinocytes, a Peak Force Tapping study on living cells. *Journal of structural biology*, 178, 1-7.

186. Uchihashi, T. and Scheuring, S. (2018) Applications of high-speed atomic force microscopy to real-time visualization of dynamic biomolecular processes. *Biochimica et Biophysica Acta (BBA)-General Subjects*, 1862, 229-240.

187. Ando, T., Uchihashi, T. and Scheuring, S. (2014) Filming biomolecular processes by high-speed atomic force microscopy. *Chemical reviews*, 114, pp.3120-3188.

188. Efremov, Y.M., Cartagena-Rivera, A.X., Athamneh, A.I., Suter, D.M. and Raman, A. (2018) Mapping heterogeneity of cellular mechanics by multi-harmonic atomic force microscopy. *Nature Protocols*, 13, 2200-2216.

189. Cartagena, A. and Raman, A. (2014) Local viscoelastic properties of live cells investigated using

- dynamic and quasi-static atomic force microscopy methods. *Biophysical Journal*, 106, 1033-1043.
190. Watanabe, H., Uchihashi, T., Kobashi, T., Shibata, M., Nishiyama, J., Yasuda, R. and Ando, T. (2013) Wide-area scanner for high-speed atomic force microscopy. *Review of Scientific Instruments*, 84.
191. Waite, J.R., Tan, S.Y., Saha, H., Sarkar, S. and Sarkar, A. (2023) Few-shot deep learning for AFM force curve characterization of single-molecule interactions. *Patterns*, 4.
192. Müller, P., Abuhattum, S., Möllmert, S., Ulbricht, E., Taubenberger, A.V. and Guck, J. (2019) Nanite: Using machine learning to assess the quality of atomic force microscopy-enabled nano-indentation data. *BMC bioinformatics*, 20, 1-9.
193. Dokukin, M. and Dokukina, I. (2020) Application of ensemble machine learning methods to multidimensional AFM data sets. *Procedia Computer Science*, 169, 763-766.
194. Minelli, E., Ciasca, G., Sassun, T.E., Antonelli, M., Palmieri, V., Papi, M., Maulucci, G., Santoro, A., Giangaspero, F., Delfini, R. and Campi, G. (2017) A fully-automated neural network analysis of AFM force-distance curves for cancer tissue diagnosis. *Applied Physics Letters*, 111.
195. Roy, R. and Desai, J.P. (2014) Determination of mechanical properties of spatially heterogeneous breast tissue specimens using contact mode atomic force microscopy (AFM). *Annals of Biomedical Engineering*, 42, 1806-1822.
196. Valero, C., Navarro, B., Navajas, D. and García-Aznar, J.M. (2016) Finite element simulation for the mechanical characterization of soft biological materials by atomic force microscopy. *Journal of the mechanical behavior of biomedical materials*, 62, 222-235.
197. Han, R. and Chen, J. (2021) A modified Sneddon model for the contact between conical indenters and spherical samples. *Journal of Materials Research*, 36, 1762-1771.
198. Deng, X., Xiong, F., Li, X., Xiang, B., Li, Z., Wu, X., Guo, C., Li, X., Li, Y., Li, G. and Xiong, W., (2018) Application of atomic force microscopy in cancer research. *Journal of nanobiotechnology*, 16, 1-15.
199. Kontomaris, S.V., Malamou, A. and Stylianou, A., 2020. A new approach for the AFM-based mechanical characterization of biological samples. *Scanning*, 2020.
200. Kontomaris, S.V., Malamou, A. and Stylianou, A. (2022) The Hertzian theory in AFM nanoindentation experiments regarding biological samples: Overcoming limitations in data processing. *Micron*, 155, 103228.